

**Crustal structure of the North Iberian continental margin from seismic
refraction/wide-angle reflection profiles.**

M. Ruiz ⁽¹⁾, J. Díaz ⁽¹⁾, D. Pedreira ⁽²⁾, J. Gallart ⁽¹⁾, and J.A. Pulgar ⁽²⁾

⁽¹⁾ Department of Structure and Dynamics of the Earth. Institute of Earth Sciences
Jaume Almera, ICTJA-CSIC. Lluís Solé i Sabarís s/n. 08028 Barcelona, Spain.
(mruiz@ija.csic.es)

⁽²⁾ Department of Geology, University of Oviedo, Arias de Velasco s/n. 33005 Oviedo,
Spain.

Abstract

The structure and geodynamics of the southern margin of the Bay of Biscay have been investigated from a set of 11 multichannel seismic reflection profiles, recorded also at wide angle offsets in an onshore-offshore network of 24 OBS/OBH and 46 land sites. This contribution focuses on the analysis of the wide-angle reflection-refraction data along representative profiles. The results document strong lateral variations of the crustal structure along the margin and provide an extensive test of the crustal models previously proposed for the northern part of the Iberian Peninsula. Offshore, the crust has a typical continental structure in the eastern tip of the bay, which disappears smoothly towards the NW to reach crustal thickness close to 10 km at the edge of the studied area (~45 °N, 6 °W). The analysis of the velocity-depth profiles, altogether with additional information provided by the multichannel seismic data and magnetic surveys led to the conclusion that the crust in this part of the bay should be interpreted as transitional from continental to oceanic. Typical oceanic crust has not been imaged in the investigated area. Onshore, the new results are in good agreement with previous results and document the indentation of the Bay of Biscay crust into the Iberian crust, forcing its subduction to the North. The interpreted profiles show that the extent of the southward indentation is not uniform, with an Alpine root less developed in the central and western sector of the Basque-Cantabrian Basin. N-S to NE-SW transfer structures seem to control those variations in the indentation degree.

Keywords: Bay of Biscay, Pyrenees, Cantabrian Mountains, hyperextended continental crust, Wide-angle seismic profiles, OBS, Alpine Orogeny.

1. Introduction

The North Iberian Margin forms the southern margin of the Bay of Biscay, opened during the Late Cretaceous and affected by contractional deformation in the Cenozoic, holding the submerged western continuation of the Northern Pyrenees. Bathymetric charts indicate the presence of an abyssal plain in the central part of the Bay of Biscay, with a basement that lacks of clear seafloor spreading magnetic anomalies eastwards of $\sim 8^\circ\text{W}$ (Figure 1). The area reveals a significant structural complexity, moving from a thickened continental crust beneath the Cantabrian Mountains (the coastal range that represents the western continuation of the southern Pyrenees) to a thinned crust near the axis of the Bay, and to oceanic crust to the west of $\sim 8^\circ\text{W}$. The zone of the Bay of Biscay investigated in this contribution constitutes an intermediate domain between the clear oceanic crust to the west (e.g. Sibuet et al., 2004), and an area of more focalized extension that gave rise to very deep sedimentary basins in hyperextended continental crust systems, leading to local mantle exhumation along the Pyrenean realm (Lagabrielle and Bodinier, 2008; Jammes et al., 2009; Lagabrielle et al., 2010; Roca et al., 2011; Tugend et al., 2014, 2015; Teixell et al., 2016; DeFelipe et al., 2017). Therefore, unraveling the structure and composition of this intermediate domain is of great interest for the study of the spatial and temporal evolution of lithospheric extension processes. Onshore, the crustal-scale structure of the Pyrenean-Cantabrian orogenic belt, in particular the pattern of indentation between the Iberian and the European/Bay of Biscay crusts, has been documented previously to the west of the studied area (Pulgar et al., 1996; Gallart et al., 1997; Fernández-Viejo et al., 1998; Pedreira et al., 2003, 2007, 2015; Gallastegui et al., 2016) but no models are available so far for the zone here investigated.

To accomplish these tasks, a broad set of new geophysical data was acquired in 2003 onboard the R/V BIO Hesperides in the framework of the MARCONI project (Spanish acronym for MARGen COntinental NordIberico -North Iberian Continental Margin-) (Figure 1). For the first time in this area, the deep crustal architecture was investigated by implementing multichannel seismic profiles (Ferrer et al. 2008; Fernández-Viejo et al., 2011) and an onshore-offshore net of wide-angle profiles using both OBSs and land stations (Ruiz, 2007).

This contribution deals with the interpretation of the wide-angle profiles that provided the most significant results, three of them oriented N-S, two E-W and a last one NW-SE. The deployment of OBS and land stations provided an excellent opportunity to obtain velocity-depth profiles across the margin to complement the structural images derived from vertical incidence seismic profiles. This information is essential to characterize the transition between the continental and oceanic crusts, which has important implications for the geodynamic evolution of the Bay of Biscay. Also, no other surveys involving ocean bottom seismometers (OBS) have been carried out up to date in this area.

2. Tectonic setting

The study area was affected by the Variscan and Alpine orogenies, separated by a large extensional period during the Mesozoic related to the opening of the Bay of Biscay and the formation of the Armorican and North-Iberian margins. The Iberian Massif is the largest outcrop of the Variscan belt in Iberia, occupying most of the western half of the Iberian Peninsula. In the studied area (Fig. 1), it offers an excellent cross section from the internal zones of the orogen (Central-Iberian and West-Asturian Leonese zones) to the foreland thrust and fold belt (The Cantabrian Zone) (Pérez-Estaún et al., 1988). The Pyrenean Axial Zone constitutes another large Variscan massif cropping out in E-W direction along the central axis of the Pyrenean range (Fig. 1). The Variscan deformation ceased in this area at the end of the Carboniferous, and by Permian times, the orogenic building was already heavily eroded and the sedimentation was mainly controlled by the development of normal faults and grabens in a new distensive regime (Jabaloy et al., 2002).

From Triassic to Late Cretaceous, this region was reworked by an extensional deformation regime related to the opening of the North Atlantic Ocean. The Bay of Biscay opened in a V-shape as a new arm propagated from the Atlantic spreading center, producing a ~35° counterclockwise rotation of Iberia with respect to stable Eurasia (Van der Voo, 1990). The exact kinematics of Iberia during this period is a matter of intense debate today (e.g. Barnett-Moore et al., 2016, and references therein) due to ambiguities in the identification of seafloor magnetic anomalies, and uncertainties in the collection of paleomagnetic data. The only clear and undisputed seafloor spreading anomalies are located to the west of 8°W: anomaly A33o, in the extinct spreading axis (dating the end of seafloor spreading at ~80 Ma) and anomalies A34, to the north and south of it (Srivastava et al., 1990; Sibuet et al. 2004). Sibuet et al. (2004) proclaimed the identification of anomalies M0-M3 at both sides of A34

and extending to ~6 °W, but their origin is highly controversial. They were first interpreted as seafloor spreading anomalies (Sibuet et al., 2004) and later reinterpreted in the contiguous West Iberian margin as created by serpentinization of exhumed mantle (Sibuet et al., 2007) or by magmatic underplating developed at the onset of breakup and affecting either serpentinized mantle or oceanic crust (Bronner et al., 2011). A similar process of gabbroic intrusions affecting serpentinized mantle was also recently proposed in a geophysical-petrological model of the North-Iberian margin around 4.5 °W (Pedreira et al., 2015).

To the east, the extension was less intense and more focalized in narrower hyperextended systems, with the development of large sedimentary basins in the Pyrenean realm and leading to the individualization of Iberia as a subplate. The Basque-Cantabrian Basin, located in the northern border of Iberia (Figure 1), is one of these basins, where more than 10 km of Mesozoic sediments were deposited over an extremely thinned continental crust (Rat, 1988; García-Mondéjar et al., 1996; Pedreira, 2005), and even locally, on top of serpentinized mantle (DeFelipe et al., 2017).

Later on, the convergence between Iberia and Eurasia in the framework of the Alpine orogeny produced the partial closure of the Bay of Biscay and the building of the Pyrenean-Cantabrian mountain belt, with the deformation of the North Iberian Margin and the northward subduction of the Iberian crust beneath the European one (Choukroune, 1992; Muñoz, 1992; Vergés et al., 1995; Pulgar et al., 1996; Teixell, 1998). The architecture of the belt was strongly controlled by the inversion of the Cretaceous extensional basins (e.g. Jammes et al., 2014; Tugend et al., 2014). The southern arm of the doubly-vergent Pyrenean chain prolonged through the Mesozoic Basque-Cantabrian Basin to the western termination of the Cantabrian Mountains, while the northern Pyrenean fold-and-thrust belt spread along the Cantabrian Margin (Gallastegui et al., 2002). The deformation in the Pyrenees started in the Late Cretaceous (Vergès et al., 1995) but it was not until Mid- to Late Eocene that it was recognizable in the Cantabrian continental margin. The estimated amount of total shortening varies from east to west: 142-165 km in the Central Pyrenees (Beaumont et al., 2000, Mouthereau et al., 2014), 75-114 km in the western Pyrenees (Séguret and Daignières, 1986; Teixell, 1998, Teixell et al., 2016), ~86 km in the eastern Cantabrian Mountains (Basque-Cantabrian Basin) (Pedreira, 2005), and ~96-98 km in the central Cantabrian Mountains and continental margin (Gallastegui, 2000; Gallastegui et al., 2002; Pedreira et al. 2015).

Onshore, the Cantabrian Mountains comprise three different structural zones: 1) The Eastern Cantabrian Mountains, developed by the inversion of the Mesozoic Basque-Cantabrian Basin during the Latest Cretaceous and the Paleogene. This zone is limited to the west by the Paleozoic outcrops of the Cantabrian Zone and extends to the north along the Cantabrian (or North-Iberian) Continental Margin. Its eastern limit is usually located at the Pamplona fault, a NE-SW striking vertical and deep structure, which played an important role in controlling the Mesozoic sedimentation (Gómez et al., 2002; Pedreira et al., 2003). Recent passive seismic data confirmed that the Pamplona Fault is a crustal-scale feature and has played a major role in the regional geodynamic history (Diaz et al., 2012); 2) the Central Cantabrian Mountains, in which the Alpine deformation lead to the exhumation of a large basement block belonging mainly to the Variscan Cantabrian Zone (Alonso et al., 1996; Fillon et al., 2016); and 3) the Western Cantabrian Mountains, in which the relief and amount of shortening diminish progressively to the Atlantic coast of Galicia (Martín-González and Heredia, 2011).

Offshore, the contractional deformation of the Alpine orogeny made the North Iberian Margin completely different from its conjugate to the north, the Armorican Margin. Whereas the Armorican margin shows a very wide (up to 175 km) continental platform and their extensional basins were only slightly inverted (Thinon et al., 2003), the Mesozoic continental platform of the North Iberian margin was uplifted to form the Cantabrian Mountains, being the present-day platform less than 30-40 km wide and giving way to the North to a steep continental slope (10-12%) with deep submarine canyons (Lastres, Llanes, Torrelavega and Santander canyons). The extinct spreading axis of the Bay of Biscay is displaced towards the South with regard to the geometrical axis of the V-shaped abyssal plain, and a thick accretionary wedge was identified at the foot of the North-Iberian slope (Alvarez-Marrón et al., 1997; Gallastegui et al., 2002; Fernández-Viejo et al., 2012). These features, together with many other geophysical observations both on land and offshore, indicate that a significant part of the basement in the Bay of Biscay was consumed beneath North-Iberia. A wide range of models have been proposed so far since the earlier interpretations of pure oceanic subduction in this area (Bacon et al., 1969; Boillot et al. 1971, Boillot and Capdevila, 1977): oceanic crust subducting immediately beneath the thinned continental crust of the margin (Álvarez-Marrón et al., 1998), subduction of transitional to proto-oceanic crust (Roca et al., 2011), underthrusting of lower crust (Gallastegui et al., 2002) and underthrusting of serpentinized mantle together with lower crustal rocks (Fernández-Viejo et al., 2012, Pedreira et al., 2015).

The easternmost sector of the investigated area includes the Parentis Basin and the Landes high. The Parentis Basin is a 100 km wide deep depression containing up to 15 km of Mesozoic, Tertiary and post-Variscan Paleozoic sediments. Beneath the basin, the Moho was uplifted 15 km with regard to the adjacent areas and the crust below the sedimentary cover was thinned to a minimum of 5 km (Marillier et al., 1988; Bois et al., 1997; Ferrer et al., 2008). The Landes High presents a very thin sedimentary cover (2-3 km thick) and a crustal thickness close to ~30 km (Marillier et al., 1988). It separates the Parentis basin from the inverted basins of the Pyrenean-Cantabrian realm and acted as an important buffer for the propagation of the contractional deformation to the North (Ferrer et al., 2008).

3. Previous Seismic Studies

To the east of the Bay of Biscay, the Pyrenees have been the aim of several deep seismic reflection (ECORS projects) and refraction/wide-angle reflection profiles (Explosion Seismology Group Pyrenees Profiles) since the end of 1970s, as shown in Figure 1 (Gallart et al., 1980, 1981; Daignières et al., 1981, 1982; Choukroune and ECORS Team, 1989; Daignières et al., 1989; Suriñach et al., 1993; Daignières et al., 1994). These studies revealed the complex deep structure of this mountain chain, with the thinner European crust indenting into the thicker Iberian one, forcing the subduction of the latter to the north and the formation of a doubly-vergent orogenic wedge at upper crustal to mid crustal levels (Roure et al., 1989; Mattauer, 1990; Muñoz, 1992; Choukroune, 1992; Teixell, 1998). This geometry has been documented later using receiver functions from teleseismic data recorded at permanent and temporal broad-band stations deployed across the Pyrenees (Díaz et al., 2012; Chevrot et al., 2015; Díaz et al., 2016) and using full-waveform inversion of data recorded along dense profiles crossing the western Pyrenees (Wang et al., 2016).

The North-Iberian (or Cantabrian) Margin at sea was the object of commercial reflection lines for oil and gas exploration and scientific studies since 1970s (e.g. Boillot and Malod, 1988), but the lithospheric structure was almost unknown until the early 1990s. The intensive crustal studies in the western continuation of the Pyrenees along the Cantabrian Mountains and continental margin started with the ESCIN (Spanish acronym for “Seismic Study of the North Iberian Crust”) project (Figure 1). That project involved two onshore and two offshore multichannel deep seismic reflection profiles, complemented by other geophysical methods such as seismic refraction/wide-angle reflection profiles and gravity modelling (Pérez-Estaún, 1994; Pulgar et al., 1996; Álvarez-Marrón et al., 1996, 1997; Gallastegui et al., 1997, 2002; Martínez-Catalán et al., 1997; Ayarza et al., 1998; Fernández-

Viejo et al., 1998, 2000). Later on, the northern part of Iberia was explored by a large E-W refraction/wide-angle reflection profile covering a total of 960 km from Galicia to the Pyrenees Chain, as well as a set of transverse profiles sampling the transition between the Cantabrian Mountains and the Duero Basin to the south. The outcomes of those projects emphasized the relationship between the Pyrenees and the Cantabrian realms as parts of a larger orogenic structure, evidencing the presence of a continuous Alpine crustal root from the Cantabrian Mountains to the central Pyrenees. The northward subduction of the Iberian crust was identified down to at least 55 km depth. Bodies of relatively high velocities (6.40 – 6.75 km/s) were also inferred at mid-crustal depths were also inferred and associated to portions of the European/North-Iberian margin lower crust indenting the Iberian crust (Pulgar et al., 1996, 1997; Gallart et al., 1997; Fernández-Viejo et al., 1998, 2000; Pedreira et al., 2003, 2007).

Offshore, Ferrer et al. (2008), Roca et al. (2011) and Fernández-Viejo et al. (2011) have investigated the seismic reflection profiles acquired during the MARCONI experiment to conclude that the Alpine compression resulted in the development of north verging thrusts at the foot of the continental slope and in the inversion of previous Mesozoic extensional structures.

4. Data acquisition, processing and modelling approach.

The oceanographic survey carried out in September-October 2003 onboard the Spanish research vessel BIO Hesperides allowed the acquisition of different sets of geophysical data, including multichannel and refraction/wide-angle reflection seismic profiles, multibeam bathymetry, and potential fields. During the first leg of the campaign, the crustal reflectivity and the velocity-depth distribution of the eastern half of the margin, between longitudes 6°W-2°W and latitudes 42.5°N-46°N, were investigated from a set of 11 seismic profiles (Figure 1). Five N-S profiles with lengths between 140 and 250 km were crossed by three E-W ones, 270-280 km long. Additionally, two NW-SE lines, of 70 and 110 km length, were acquired in the western and eastern edges of the study region, respectively. Finally, a 40 km long E-W profile was shot close to the shoreline over the central sector of the continental platform. In total, more than 2000 km of profiles were acquired. An onshore-offshore network of 24 Ocean-Bottom Seismometers or Hydrophones (OBS/OBH) and 35 land stations deployed in

46 different sites (Figure 1) was operated to record the seismic signals and provide information on seismic velocities.

The OBS/OBH network remained fixed during all the experiment and covered on place the complete the profile intersections, with an average spacing of 30-40 km. This approach resulted in a rather low instrumental density, but allowed to infer a first approximation to the regional scale image of the velocity-depth distribution. The land seismic stations were deployed with an average spacing of 10-15 km extending the N-S profiles onshore, with some additional instruments following the shoreline (Figure 1).

The seismic source consisted of a Bolt airgun array fired every 40 s, resulting in a shot spacing of 100 m, which is a compromise between the requirements of the multichannel reflection and the wide-angle seismic methods. The shooting pressure was set constant at 140 bars but, due to mechanical problems, the air gun volume varied from 2690 in³ to 1435 in³ depending on the profile. Regarding oceanic instruments, both Ocean Bottom Seismometers (OBS) and Ocean Bottom Hydrophones (OBH) were used. Most of them (12 OBS and 8 OBH) were provided by the Leibniz Institute of Marine Sciences, Kiel (IFM-GEOMAR), while the remaining 4 OBS belonged to the Spanish Marine Technology Unit (UTM-CSIC). The OBS were equipped with a three-component short period seismometer and a hydrophone, and recorded data with a sampling rate of 250 sps, whereas the OBH were equipped only with a hydrophone and worked with a sampling rate of 200 sps. On land, instruments from the Institut de Physique du Globe de Paris (IPGP), the University of Oviedo and the Institute of Earth Sciences 'Jaume Almera' (ICTJA-CSIC) were used. All the stations were equipped with three-component seismometers, most of them of short period type (1-2 Hz) even though some intermediate band instruments (Le20s) were also used. In all cases the stations were operated in continuous recording mode with a sampling rate of 100 sps and GPS synchronization.

Processing of the OBS/H data included calculation of the internal clock drift corrections. The mean drift for all instruments was 2.5 ms per day, with maximum and minimum values of 9.0 ms/day and 0.3 ms/day, respectively. The OBS/OBH positions were 2D/3D relocated by analysing the direct arrivals. The mean spatial drift was less than 100 m, being 304 m the maximum correction and 11 m the minimum. Filter panels with narrow frequency band passes were constructed to determine the frequencies of the seismic signal, showing that they are contained in the 3-17 Hz range. For offsets smaller than 105 km, an

Ormsby zero-phase band-pass filter with corner frequencies at 5 and 12 Hz was applied to the raw signals, while for offsets greater than 105 km the filter was closed to 5-8 Hz to take into consideration the attenuation of the higher frequencies. A Wiener deconvolution was also applied to improve the temporal resolution of the seismic data. The best resolution was obtained for a predictive length of 50 ms, an operator length of 200 ms and dividing each trace into 3 s data gates with 1 s overlap. As a second step in the processing of the OBS/H data, a frequency-wavenumber (F-K) filter was used to suppress the strong arrival related to the source direct wave and the amplitudes of the previous shots. Finally, a frequency-dependent lateral phase coherence filter (Schimmel and Gallart, 2007) was applied to enhance the coherent components of the seismic records by attenuation of incoherent noise. The use of this filter critically improved the identification and correlation of seismic phases to larger offsets, as documented in the Supplementary Figure S1, presenting the record sections before and after filtering for an OBS and a land station. Except for the clock drift correction, land stations record sections were processed in a similar way, by applying a 3-15 Hz band-pass and a frequency-dependent lateral phase coherence filters.

For the following record sections, refractions through the sedimentary cover, the upper crust and the upper mantle are labelled as Ps, Pg and Pn, respectively. PiP, PcP and PmP, denote reflections at the top of the middle crust, the top of the lower crust and the Moho discontinuity, respectively. We must stress that by “lower crust” we are using a geophysical rather than a geological definition, as we refer to a layer with velocities ranging between ~6.5 km/s and the typical mantle velocities of ~8 km/s, independently of the crustal or mantle origin for the rock types that compose it. Additional wide-angle reflections identified in some stations of the N-S sections, labelled as PcP_I and PmP_I, refer to reflections at the top of the subducting Iberian lower crust and the Iberian Moho, respectively.

After identifying the seismic phases, the P wave velocity-depth models were obtained by forward modelling of travel times and amplitudes of diving and reflected waves using the RayInvr software (Zelt and Smith, 1992). Tests using a first and secondary arrival inversion scheme (Korenaga et al., 2000) were also done, but the instrument spacing, structural complexity and data quality did not allow to obtain stable solutions. The seafloor surface and the first-order geometry of the sedimentary basins recorded from multibeam bathymetry and the multichannel seismic reflection acquired along the same profiles (Ferrer et al., 2008, Fernández-Viejo et al., 2011) have been used to define the upper layers in our models, as the wide angle data do not provide enough resolution to resolve them. Other geophysical data,

including gravimetry and previous seismic wide-angle reflection/refraction models have been used to constrain the final models in our forward modelling scheme (Fernández-Viejo et al., 2010, Pedreira et al., 2007). The integration of this information has proved to be very useful in order to provide a better structural constraint, hence reducing the ambiguity in the final model (Zelt, 1999).

5. Data description and modelling results

5.1. N-S Profile MARCONI-1

The MARCONI-1 N-S profile is the longest line acquired during the survey, with a total length of 330 km, 250 km of which are coincident with the multichannel seismic profile. The velocity-depth model for this profile extends from the Cantabrian Zone to the beginning of the continental slope of the Armorican margin, crossing the highest peaks of the Cantabrian Mountains, the Cantabrian continental platform, the Lastres and Llanes Canyons, the Le Danois Bank and the abyssal plain. Seven land stations (B1 to B7) and five OBS/H (OBS06, OBH07, OBS08, OBS19 and OBH20) were deployed to record the refractions and wide-angle reflections (Figure 1). Most of the profile was acquired with the air guns working at full power, so land stations were able to record seismic phases for offsets greater than 220 km. The southern (OBS06) and northernmost (OBH20) marine stations, together with the one located at the foot of the slope (OBS08) allow to identify seismic phases for offsets up to 100 km (Figure 2), but the other two instruments only detected phases for offsets shorter than 60 km.

The results obtained in previous refraction surveys have been taken into account during the modelling of the land sector (Figure 1). The E-W land profile acquired in 1997 (Pedreira et al., 2003) cuts the MARCONI-1 profile perpendicularly between land stations B4 and B3. One of the profiles acquired during the 1992 survey to investigate the transition between the Duero Basin and the Cantabrian Zone (Pulgar et al., 1996; Gallart et al., 1997; Fernández-Viejo et al., 2000), crosses the Cantabrian sector in a N-S direction sub-parallel to the MARCONI land stations. Other geophysical information considered when constructing the velocity model include the results derived from the normal-incidence seismic reflection profile ESCIN-2 (Pulgar et al., 1996, 1997), parallel to the southernmost sector of the MARCONI-1 profile, and the onshore-offshore gravimetric profiles modelled along the

Cantabrian margin (Pedreira et al., 2007), all oriented parallel to the N-S MARCONI profiles up to the latitude of the E-W MARCONI-8 profile. In the marine sector, the multichannel seismic line acquired simultaneously to the wide-angle profile (Fernandez-Viejo et al., 2011; Roca et al., 2011) and the intersection with the E-W MARCONI profiles have also been considered.

Record sections of the northernmost instruments of the MARCONI-1 profile (OBS08 to OBH20) show phases related to the deepest parts of the crust, PcP and PmP, appearing at offsets smaller than 40 km, as well as Pn phases appearing at offsets of 60-100 km (Figure 2). The short time delay of these features allow inferring a thinned crust beneath the abyssal plain at the northern edge of the profile, with a crustal thickness close to 10 km. The final velocity-depth model (Figure 6a) shows that this thinning is essentially affecting the middle crustal layer, which is well defined in the south but vanishes smoothly to the north. The upper crustal basement, with velocities of 5.4-5.5 km/s, is laying directly on top of the lower crust, which shows velocities of 7.2-7.3 km/s, significantly higher than expected for typical continental crust (Christensen and Mooney, 1995).

OBS08, located at the foot of the continental slope, shows asymmetric arrivals between phases coming from each side (Figure 2b). To the north, rays sample the strongly thinned crust with its anomalous velocities. Deep phases, PcP and PmP, are observed at close offsets and the Pn phase is recorded at offsets of 80-100 km in this sector. Although a precise control on the uppermost mantle velocities is not possible as Pn arrivals are not identified in the reversed profile, the interpretation of the Pn phases recorded at OBS08 and the PmP phases identified in nearby instruments, strongly support a model with a continuously thinning crust and a mantle velocity of 7.9 km/s. South of OBS08, the recorded seismic phases are strongly affected by the abrupt variation of the water column, but the PcP phase, preceded by the Pg and PiP phases, is observed at offsets of 15 to 50 km thus allowing to document the gently southward dip of the main interfaces (Figure 6a).

The record sections of the northernmost land stations (B1 to B4) show, following the arrivals related to the upper crustal structure, two phases identified as PcP and PmP (Figure 3). These phases together with the ones recorded at the southernmost OBS allow to constrain the top and the bottom of the Bay of Biscay lower crust, delimiting the geometry of the indentation structure. The Moho deeps progressively to the south and presents its maximum depth beneath stations B2 and B3, where it reaches 29 km depth. Pedreira et al. (2015) have

shown that this imbrication between the Bay of Biscay crust and the Iberian crust is consistent with a model constructed down to 400 km depth following a geophysical-petrological approach that calculates a realistic distribution of densities and seismic velocities in each node of the mantle and the subducting Iberian lower crust, according to its chemical composition, pressure and temperature. The model fits Bouguer gravity anomalies, geoid undulations, surface heat flow, elevation and seismic velocities. The lower crust appears as a thin layer, less than 5 km thick, in most of the marine region, but the top of the lower crust rises progressively to the south when approaching the shoreline. The top of the lower crust is located at 20 km depth beneath OBS06 and becomes progressively shallower to the South, reaching 14 km depth between stations B3 and B4. The velocities of the lower crust range from 6.4-6.5 km/s in the southern indenter wedge to 6.9-7.0 km/s beneath the continental platform. A middle crust layer, with velocities between 6.0 and 6.25 km/s is identified beneath the continental platform, with a thickness around 7 km beneath station B2 and progressively thinning to the North.

Pn phases are in general weak for most of the investigated profiles. The exceptions of this rule are the strong arrivals observed in the northernmost land stations along profile 1. The phase interpreted as Pn covers more than 120 km for some of those stations (Figure 3a). Because of its strong energy it could be erroneously identified as a PmP, but the travel times predicted for the reflection on the Bay of Biscay Moho, well constrained by the OBSs arrive with a delay of approximately one second at the offsets where the strong phase begins. We interpret the large Pn amplitude at those stations as the result of the steady thinning of the Moho to the North, that produces a focusing effect on Pn phases. Fernandez-Viejo et al (1998) have shown a beautiful example of a similar feature, stating that a station located close to the shoreline, samples the thin, European crust while an innermore site samples both Iberian and European crust and results in much lower Pn amplitudes. PmP phases from both types of crust are also clearly shown there. We consider we are evidencing an equivalent situation in our Profile 1, although the differences are less clear in our data set, probably due to the lower energy of the airguns employed. The slope of this Pn phase, with the mentioned constraints on the Moho depth, indicates an upper mantle velocity of 7.9 km/s. The control on the upper mantle velocity is not as good as it would be with the identification of Pn phases in reversed shots, but the mentioned geophysical-petrological modeling of Pedreira et al. (2015) along a near coincident line shows that the low velocity values proposed for the uppermost mantle in our models is consistent with the rest of geophysical observations.

The southernmost land station (B6) shows at their minimum offsets series of arrivals that have been identified as reflections at the top and bottom of the Bay of Biscay lower crust, PcP and PmP phases respectively (Figure 3b), allowing to constrain this structure in the indentation zone. Following these onsets, approximately 1 second after the PmP, a later arrival has been identified (labeled PcP₁), which cannot be explained with the geometry of the Bay of Biscay lower crust constrained by the OBS and northern land stations. A discontinuity deeper than the Bay of Biscay Moho and deeping to the north has to be introduced in the model to account for these observations. Reflections on this discontinuity are also responsible of the far arrivals detected at offsets of 235-280 km, which cannot be explained as a refraction in the upper mantle because the Pn phase arrives approximately 1s before at offsets of 180-220 km (Figure 3b). Using constraints from previous refraction profiles on land (Pedreira et al., 2003), we interpret this interface as the top of the subducting Iberian lower crust. Southwards of the slope deformation zone (at offsets 150-170 km), some traces suggest even a later phase arrival that could be interpreted as arising from the Iberian Moho. Although these arrivals are not particularly clear in these record sections, they could be easily accounted for with a Moho geometry similar to that proposed for the wide-angle recordings of the ESCIN-4 profile located 40 km westward (Pulgar et al., 1996; Gallart et al., 1997; Fernández-Viejo et al., 1998) and imaging an Iberian crust deepening down to 55 km depth. The position of the Iberian Moho is also compatible with the one determined along the intersecting E-W land profile P01 (Pedreira et al., 2003).

5.2. N-S Profile MARCONI-3

MARCONI-3 is the easternmost N-S profile and has a length of 240 km, 143 km of which are located offshore coincident with the multichannel seismic profile (Figure 1). It departs in the south from the Basque-Cantabrian basin and crosses the Landes high and the Parentis basin, cutting the Capbreton and Cap Ferret canyons perpendicularly. The airgun shots were recorded by 8 land stations (D1 to D8), approximately with a 10 km spacing, and 4 marine stations (OBS13, OBH14, OBS15 and OBS16), deployed every 35-40 km (Figure 1). The data quality of this profile is in general very good, being possible to detect seismic phases at offsets reaching 120 km.

The multichannel seismic profile (Ferrer et al., 2008), obtained simultaneously to the wide-angle one, has been used to constrain the geometry of the sedimentary basins in the marine sector. Onshore, the 1997 E-W profile 1 (Pedreira et al., 2003) was considered when

modeling the Iberian crust. It must be noted that the intersection between both profiles is situated over the Bilbao Anticline, a zone with an important positive gravity anomaly (Casas et al., 1997; Pedreira et al., 2007) and the strongest aeromagnetic anomaly of the Spanish mainland (Ardizzone et al., 1989), evidencing the presence of magnetic and anomalously dense bodies at shallow depths (Aller and Zeyen, 1996; Pedreira et al., 2007).

The OBS and land stations D1 to D6 (Figure 4a and 4b) allowed to characterize the crustal discontinuities of the upper, middle and lower crust of this sector of the Bay of Biscay. The Moho in the Bay of Biscay produces very clear and strong reflections, observed at offsets up to 100-125 km. It is located at less than 20 km depth beneath the Parentis Basin, deepening to the south until reaching 33 km depth beneath the shoreline, where it raises again progressively to the south (Figure 6b). The top of the lower crust is situated at 16 km depth under OBS16, deepening to the south and reaching its maximum depth of 22.5 km beneath OBH14, where it starts rising again and reaching 16.8 km depth beneath land station D3. The Bay of Biscay middle crust presents velocities comprised between 6.1-6.3 km/s, and the lower crust show values of 6.65-6.9 km/s.

Phase arrivals recorded at offsets 110-130 km and reduced times of 8.5 s and 10 s at station D7 (Figure 4c) show approximately 2s delay with respect to the PcP and PmP of the Bay of Biscay crust recorded at northern land stations at similar offsets. As for the MARCONI-1 profile, these phases are interpreted as reflections at the top and base of the Iberian lower crust, which deeps to the north, hence depicting the subduction of the Iberian crust beneath the Bay of Biscay crust. The southernmost station, D8, show similar phases that can be interpreted consistently. The E-W Profile 1 model of Pedreira et al., (2003, see Figure 1) shows the presence of a high velocity body located between 10 and 12 km depth in the region intersecting with the MARCONI-3 profile. This body has been interpreted as a portion of the Bay of Biscay lower crust raised at shallower depths by Alpine structures with northward vergence, and responsible for the gravity and magnetic anomalies observed over the area (Pedreira et al., 2007). Since the shooting of the MARCONI-3 profile was done exclusively offshore, the large offset for land station D7 does not allow to constrain the geometry of this body or to rule out its presence. Therefore, this body has been arbitrarily introduced in the velocity-depth model at the crossing point with the E-W Profile 1, only to be coherent with the previous results and to document that the new observations are compatible with its presence.

5.3. E-W Profile MARCONI-4

MARCONI-4 is the northernmost E-W line acquired during the survey. With a total length of 267 km, it runs across the central part of the Bay of Biscay, crossing the deepest part of the abyssal plain and the Landes high along the southern slope of the Cap Ferret canyon (Figure 1). Multichannel and wide-angle seismic data superimpose over the total line length. A total of 7 sea bottom stations (OBS04, UTM01, OBS19, UTM04, OBS18, OBH17 and OBS16) were deployed with a mean spacing of 40-45 km, but unfortunately OBS04 and UTM04 were not recovered at the end of the survey. OBS04 was found on 2011, 8 years after its deployment, aground on a Biscay cove and still containing good quality data, but UTM04 seems to be definitively lost. Due to the sampled structure, recorded seismic phases do not exceed offsets greater than 50 km on most of the stations. Nevertheless, PcP and PmP can be clearly identified, allowing to constrain the crustal structure of this region. OBS04 detects an arrival at offsets reaching 140 km, which has been identified as the Pn phase, providing information on the mantle velocity (Figure 5).

The models derived from the recorded data allows to establish important differences between the crustal structure of the Landes High and the abyssal plain. The record sections of the two OBSs located along the Cap Ferret Canyon slopes do not allow to identify PmP nor PcP phases. The deeper part of the velocity-depth model (Figure 6c) uses in this zone the geometry and velocities derived from the analysis of the intersecting MARCONI-3 profile, with a Moho located at 20 km depth and a 3 km thick lower crust with velocities of 6.8-6.9 km/s. The eastern segment of Moho sampled by MARCONI-4, located between OBH17 and OBS18, is located at this same depth (Figure 6c). An independent confirmation of the Moho depth in the north-eastern sector of the investigated area arises from the interpretation of profile MARCONI-7, running NW-SE and intersecting profile MARCONI-4 at OBH17 (Figure 1). The Moho depth in this area is also constrained by a strong PmP phase in the record section of OBS18 to the west (Figure 5a). The middle crust is well-defined, with its top located around 10 km depth and velocities ranging between 6.1 and 6.3 km/s (Figure 6c).

The record sections of the OBSs deployed in the western sector depict, coherently with what happened in the northern edge of the MARCONI-1 N-S profile, PcP and PmP phases appearing at offsets smaller than 40 km (Figure 5b and 5c). Data analysis shows a thinned crust in this area, with a velocity-depth distribution characterized by anomalously low velocities in the upper and middle crust region, contrasting with high velocities in the lower

crust. In this sector of the profile the Moho has been constrained at approximately 17 km depth, the crustal thickness being less than 13 km (Figure 6c). The lower crust presents velocities of 6.9-7.0 km/s in the central sector of the profile, but reaches 7.3-7.4 km/s in its western end. The layer above it presents velocities of 5.4-5.5 km/s around the crossing point with the N-S MARCONI-1 profile and it decreases to approximately 5.3 km/s in the western edge. Mantle velocities, constrained by the diving phases recorded at offsets between 90 to 140 km in OBS04 (Figure 5c), are 7.8-7.9 km/s, coherently with values observed along the MARCONI-1 profile. Those values are lower than the mantle velocities derived for the eastern section of the profile, ranging between 8.0 and 8.1 and hence close to typical ocean upper mantle (Figure 6c). The westernmost N-S profile acquired in this survey, MARCONI-5, provides independent confirmation of the crustal structure of this sector, with a Moho located at 25 km depth south of OBH02 and thinning northwards to reach 16 km depth in the northern edge the profile. The lower crust sampled by this profile shows a northward increase in the velocity, from 6.7-6.8 km/s beneath OBS01 to 7.3-7.4 km/s in the northern edge (Supplementary Figure S2).

40 km south of MARCONI-4, MARCONI-8 profile (Supplementary Figure S2), also oriented E-W, sample the central part of the Landes High and the southern border of the Bay of Biscay abyssal plain. As for profile MARCONI-4, data show a clear east-west change in the crustal properties (Figure 7). To the East, the top of the lower crust and the Moho is located around 18 and 24 km depth, respectively. In this region, the lower crust shows velocities of 6.8-6.9 km/s, while a typical continental middle crust with velocities ranging from 6.0 to 6.3 km/s is evidenced. Further West, data allow to constrain a Moho rising smoothly up to 16.5 km depth at the western termination of the profile. Consistently with profile MARCONI-4, the thickness of the lower crust is reduced towards the west and the increase in the lower crustal velocities, up to 7.2-7.3 km/s, is followed by rather low velocities, of 5.4-5.6 km/s, in the middle crust.

5.4 Models uncertainty and resolution

The uncertainty associated to wide angle reflection/refraction models is difficult to document accurately, in particular when only forward modeling can be used. Different factors, including the subjective uncertainty in the picking of travel times, the ray coverage in the different parts of the model and the misfit between calculated and theoretical travel times should ideally be considered. Even if different suggestions have been proposed for indirect

model evaluation (Zelt and Smith, 1992, Loureiro et al. 2016) the methods are difficult to implement, in particular for models including layers that pinchout. In order to provide an insight on the potential errors of our models, we have first evaluated the quality of the fit between the predicted and observed traveltimes by calculating the rms error and the associated chi-square parameter, defined as the root-mean-square misfit between observed and theoretical arrival times, normalized to the picking uncertainty. We focus our analysis on the mid and lower crustal phases, as the station spacing does not allow an accurate imaging of the sedimentary layers, that, as stated previously, have been derived from MCS profiles and other geophysical data. Table 1 show the values obtained for the three models here discussed. The lower results of the chi-square parameter, are obtained for the E-W profile 4. The values derived for the two N-S profiles are high for experiments using dense arrays of shots and receivers, but similar values have been reported for classic wide-angle reflection / refraction experiments (e.g. Zelt and Smith, 1992). Factors contributing to these high chi-square values can include out-of-plane structural and velocity variations, misidentification of some of the phases or the effect of unconstrained trade-off between velocity and boundary depths.

Zelt (1999) proposed a resolution analysis based on the measurement of the number of rays passing through a region of the model constrained by one single velocity node. However, such kind of analysis is difficult to implement in complex models. Several contributions have shown that the model areas with dense ray path coverage are basically coincident with the areas considered well resolved using Zelt's test (e.g. Mihoubi et al., 2014, Moulin et al., 2015) and hence, the ray path density can be considered as a proxy of the model resolution. We present at Supplemental Figure S3 the modeling ray paths coverage for the analyzed profiles. In profiles 1 and 3, the marine zones are clearly best sampled than the continental ones due to the geometry of the experiment. The geometry of the deep crustal reflectors is consistently constrained by rays arriving at different stations. Regarding profile 4, oriented E-W and recorded only at OBSs, has a rather good ray coverage to the West of OBS17, while its eastern termination is less constrained. Profile 3 has also a good coverage along its central part, while its northern termination is unconstrained by the seismic data.

6. Discussion: The 3D structure of the North-Iberian margin.

Results obtained in this study reveal the structural complexity of the North-Iberian margin, which presents important lateral variations inherited from the Mesozoic extensional

history and the subsequent Alpine orogenic process. In the following sections, we will discuss in more detail the characteristics of the different structural regions covered by the MARCONI survey. In short, three broad zones can be differentiated in terms of basement internal structure and Moho depth (Figures 1, 7). Zone A is composed of stretched continental crust, with Moho depths ranging from ~30 km to around 20 km and encompasses a large portion of the investigated area. Zone B, covers the NE edge of the investigated zone and corresponds to areas with Moho depths of less than 20 km and a high velocity (~7.20-7.40 km/s) lower crust. Finally, Zone C, located mostly onland, is composed of continental crust thickened during the Alpine orogenic event.

6.1. Zone A

Zone A occupies most of the southern and eastern parts of the investigated area (Figure 1). The velocity-depth features can be associated to a slightly thinned continental crust, where upper, middle and lower crustal layers are seismically well defined (Figure 6a). The MARCONI profiles sample the westernmost edge of the Parentis basin, the Landes high and the continental slope, revealing a significant crustal thinning towards the North. This feature is consistent with the previous results from the ECORS-Bay of Biscay profile, running N-S slightly eastwards of the zone here investigated (Marillier et al., 1988; Bois et al., 1997). The Moho is located at an average depth of ~30 km south of the Landes high, beneath OBH14, and decreases to about 20 km beneath OBS16, in its northern border. The eastern part of the E-W profile MARCONI-4 also samples this highly thinned domain, with an almost constant Moho depth close to 20 km.

This domain presents a well-defined middle crust, where velocities range from 6.0 to 6.3 km/s, followed by a lower crust with velocities of 6.8-6.9 km/s and topped by an upper crust with velocities of 5.80-6.00 km/s. All these values are typical for continental crust (Rudnick and Fountain, 1995; Christensen and Mooney, 1995). Preliminary results derived from the MARCONI-7 (Figure 1) profile also confirm these characteristics of continental crust, with well-defined upper, middle and lower crustal levels. This region was heterogeneously affected by the Mesozoic extensional processes, which focused the thinning of the crust in two important basins separated by the Landes high: The Parentis Basin to the north, and the Basque-Cantabrian Basin to the south. It was also heterogeneously affected by the Pyrenean contractional deformation, which was concentrated in the Basque-Cantabrian Basin. The North-Pyrenean frontal structure propagated along the Capbreton canyon and the

Landes High acted as an important buffer for the propagation of the contractional deformation to the north (Ferrer et al., 2008; Roca et al., 2011).

6.2. Zone B

Zone B occupies the central part of the Bay of Biscay and is defined by Moho depths of less than 20 km, corresponding to crustal thicknesses of 10-15 km beneath the abyssal plain. The lower crust has an almost constant thickness of about 4 km, while the middle crust progressively vanishes towards the north and west, accommodating most of the crustal thinning. The uppermost layer present velocities below 5.5 km/s while the lower crust has high velocities, reaching 7.2-7.4 km/s. The typical structure of a continental crust, differentiated in upper, middle and lower levels (Mooney et al., 2002) is not recognized in this area. This velocity-depth structure is not far from what is considered a typical oceanic crust (a 2-3 km thick sedimentary layer overlaying a 3 km thick layer with velocities ranging between 4 and 5.5 km/s and a 3-5 km thick lower crust with velocities of 6.5-7.5 km/s; (White et al., 1992; Minshull, 2002). However, there are some differences when looking at the velocity structure in detail (Figure 8). The upper layer within the basement has greater thickness and a less pronounced vertical gradient than the oceanic layer 2 in Atlantic crusts of similar age. Additionally, the lower crustal layer has weaker gradients and slightly higher velocities (especially in the upper part) than oceanic layer 3, and the mantle beneath it has lower velocities (7.8-7.9 km/s) than “normal” oceanic upper mantle. Even if those differences are not conclusive, additional observations argue against the oceanic character of the crust in this area. Firstly, the sedimentation pattern shown by the MARCONI-1 and MARCONI-11 multichannel seismic profiles, including numerous normal faults and half-graben structures (Fernández-Viejo et al., 2011), is typical of continental extensional processes and never appear in the oceanic crust (Ruppel, 1995; Cho et al., 2004). Neither a highly irregular and diffractive basement nor a generalized highly reflective Moho are observed, both being major features of an oceanic crust present in profiles acquired farther west, i.e.: ESCIN-3.1, IAM9 and IAM12 (Álvarez-Marrón et al., 1996 and 1997; Pickup et al., 1996; Fernández-Viejo and Gallastegui, 2005). Secondly, undisputed oceanic magnetic anomalies created by seafloor spreading are only present to the west of 8°W (A33o and A34, Figure 1), and the more controversial M0-M3 anomalies, considered as being created either by oceanic seafloor spreading (Sibuet et al., 2004) or by serpentinized mantle (Sibuet et al., 2007), were only identified to the west of 6°W, outside of the area studied in this contribution.

High velocities in the lower crust are characteristic of ocean-continent transition (OCT) zones in many magma-poor margins. The nature of the crust in these OCTs is highly debated, since neither the velocity structure nor the characteristics of the magnetic anomalies seem to be conclusive. These high-velocity zones have been interpreted either as thinned and intruded continental crust (Tucholke et al., 1989), as oceanic crust formed at slow/ultra-slow spreading rates (Whitmarsh and Sawyer, 1996; Srivastava and Roest, 1999) or as exhumed and serpentinized mantle that can reach the seafloor before the complete lithospheric breakup (Boillot et al., 1989; Pickup et al., 1996; Brun and Beslier, 1996; Péron-Pinvidic and Manatschal, 2009, among others). A high velocity lower crustal layer has been documented further west in the Bay of Biscay, in the OCT of the conjugate Armorican margin. That layer shows velocities of 7.4-7.5 km/s and is located beneath a basement of 5.2 km/s and immediately on top of a mantle with typical velocities of 8.0-8.1 km/s (Thinon et al., 2003). In that particular case, the high velocities were interpreted as most probably due to the presence of hydrated (serpentinized) mantle, although an undercrusted body of mafic igneous rocks was not completely excluded (Thinon et al., 2003).

In the western part of the area investigated in the MARCONI project, the velocities in the Bay of Biscay upper mantle are in the range 7.7-7.9 km/s (Fig. 6), consistently with the results derived from the ESCIN-4 profile, located 40 km to the west (Pulgar et al., 1996; Gallart et al., 1997; Fernández-Viejo et al., 1998). These velocities are slightly below typical values (8.0-8.1 km/s), suggesting some degree of mantle hydration. Velocities in the lower crust are range between 7.2 and 7.4 km/s. These values can be associated to hydrated and serpentinized mantle (e.g. Roca et al., 2011). However, the subtle velocity gradient within the lower crust and the relatively sharp velocity contrast between this layer and the ones above and below it, with clear Moho reflections at its base along profiles Marconi-1 (Figure 2a), western Marconi-4 (Figure 5b) and ESCIN-4 (Gallart et al., 1997), argues against this interpretation, at least without further clarifications. Serpentinization tends to decrease gradually with depth as less water enters into the mantle, inducing a gradual increase in seismic velocities up to normal upper mantle values and lack of clear Moho reflections (e.g. Chian et al., 1999; Dean et al., 2000). This can be observed clearly in the basement of the West Iberian margin, where velocities in the crust-mantle transition are clearly associated to the presence of serpentinized mantle, sampled by the Ocean Drilling Program Legs 103, 149 and 173 (Light purple areas in Figure 8). Hence, we propose that the high velocities in the lower crust can be tentatively related to intrusions of mafic rocks in a partially exhumed and serpentinized mantle overlaid by an extremely thinned continental crust (e.g. Pedreira et al.,

2015). We must note that in any passive margin, even if it is of “non-volcanic” type, some magmatic material is expected to be added to the crust as a result of decompression melting in the mantle. This is the reason why rifted margins are preferentially classified today as “magma-dominated” and “magma-poor” instead of “volcanic” and “non-volcanic” (Sawyer et al., 2007; Reston, 2009). Numerical models by Pérez-Gussinyé et al. (2006) predict 2-4 km of melt thickness for the stretching velocities inferred in the Bay of Biscay, and that this process takes place after serpentinization of the upper mantle (Pedreira et al., 2015). Some evidences of magmatism are observed in the study area, the most evident of which is a thick volcanic sequence, Albian to Santonian in age (Montigny et al., 1986) cropping out in the Basque-Cantabrian basin inland. Offshore, basalts were dredged in the northern slope of Le Danois Bank, as clasts within Early Cretaceous syn-rift conglomerates. Although their age is unknown, they are probably related to the rifting stage (Capdevila et al., 1980). Also, volcanic edifices were recognized in nearby areas of the Armorican margin, to the north of Profiles MARCONI-1 and 5 (Thinon et al., 2003). Intrusion of gabbroic material at the base of thinned crust and within the serpentinized upper mantle is able to explain the seismic velocities of 7.2-7.3 km/s, the rather constant thickness of this layer, the presence of Moho reflections at its base, and the values of ~7.7-7.9 km/s found beneath the Moho, which would correspond to the deeper and less hydrated part of the pre-existing layer of serpentinized mantle (Pedreira et al., 2015).

We conclude that the basement in this sector is most probably transitional continental crust, highly stretched and thinned, lying on top of serpentinized mantle and intruded by gabbroic igneous rocks at its base and within the uppermost mantle. This suggest that the lithospheric extension related to the opening of the Bay of Biscay was not enough in this area to produce a total break-up of the lithosphere before the tectonic regime changed from extensional to compressional (onset of the Alpine orogeny).

6.3. Zone C

Zone C is located to the south of the coastline and it is characterized by a thickened continental crust as a consequence of the contractional deformation between the Iberian and European plates during the Cenozoic, creating a north-directed crustal root reaching depths of 50-60 km.

The magnetic map of the Bay of Biscay (Figure 1) clearly shows the A33o-A34 and M0 anomalies displaced to the south of the geometrical axis of the western part of bay, evidencing

that its seafloor has been partly consumed. Two groups of models have been proposed during the last decades to explain this observation. On one hand, those invoking a southward oceanic subduction of the Bay of Biscay crust (Jones and Edwing, 1969; Turner, 1996; Álvarez Marrón et al., 1997; Ayarza et al., 2004; Sibuet et al., 2004), and on the other, those based in a southward displacement and underthrusting of the Bay of Biscay lower crust indenting into the Iberian crust, producing its delamination and the northward subduction of its lower part (Pulgar et al., 1996; Gallart et al., 1997; Fernández-Viejo et al., 1998, 2012; Gallastegui, 2000; Pedreira et al., 2003, 2007, 2015).

The southward oceanic subduction was proposed as it was the most logical attempt to accommodate the displacement between the Iberian and European plates and to explain the important deformation in the continental platform and the abrupt continental slope of the North-Iberian Margin. During the 80s, the seismic evidence for the northward subduction of the Iberian crust beneath in the Pyrenees was conclusive (Gallart et al., 1981; Choukroune and ECORS Team, 1989; Muñoz, 1992; Teixell, 1998). Therefore, complex models involving a change in the polarity subduction from the Pyrenees to the North-Iberian margin were required to conciliate the northward Pyrenean and the proposed southward Bay of Biscay subductions (Turner, 1996). Later on, during the 90s, several seismic profiles of the ESCI-N and related projects revealed conclusively that the Iberian crust was also subducting to the north along the Cantabrian Mountains, and that the Moho of the margin remains at shallow depths. This point, altogether with other observations concerning the internal structure of the thickened part of the crust, led to the development of the second set of models, proposing a southward displacement and underthrusting of the Bay of Biscay lower crust, indenting into the Iberian crust (Pulgar et al., 1996; Fernández-Viejo et al., 1998, 2000; Gallastegui et al., 2002; Pedreira et al., 2003, 2007, 2015). This displacement would produce the Bay of Biscay asymmetry by consuming part of the crust of the margin. The shortening of the North-Iberian platform, its steep slope and the highly deformed zone would also be generated by the development of northward verging structures during the southward advance of the lower crust (e.g. Fernández-Viejo et al., 2012). Finally, the indentation produces the delamination of the Iberian crust delamination and the northward subduction of its middle and lower parts. 3D gravimetric models (Pedreira et al., 2007) and multiobservable numerical modeling integrating geophysical and petrological data (Pedreira et al., 2015) are consistent with this hypothesis, also supported by magnetotelluric (Pous et al., 2001) or passive seismic data (Diaz et al., 2003, 2009, 2012).

The wide-angle phases recorded by the OBS and northernmost land seismic stations deployed at the MARCONI N-S profiles, allowed to continuously image the indentation geometry of the Bay of Biscay lower crust within the Iberian crust along the Cantabrian Mountains. The identification, at the southernmost land stations, of deep seismic phases showing significant time delays which are not explainable with the geometry and depth of the Bay of Biscay Moho constrained by the northern instruments, forced the introduction of one discontinuity deepening to the north, interpreted as the top of the subducting Iberian lower crust. Arrivals reflected at deeper interface, interpreted as the Iberian Moho, are difficult to identify in the MARCONI dataset, but are very clear 40 km to the west along the ESCIN-4 profile (Pulgar et al., 1996; Gallart et al., 1997; Fernández-Viejo et al., 1998). Therefore, the whole seismic dataset documents the indentation of the Bay of Biscay crust and the northward subduction of the middle and lower Iberian crust down to depths around 50-60 km along the eastern and central sector of the North-Iberian margin. The obtained models allow connecting the results in the western part of the Bay of Biscay (Pulgar et al., 1996; Gallart et al., 1997; Fernández-Viejo et al., 1998, 2000; Fernández-Viejo and Gallatogui, 2005) with those beneath the Pyrenean Chain (Muñoz, 1992; Choukroune, 1992; Teixell, 1998) and thus give additional support for the onland E-W velocity-depth model proposed by Pedreira et al. (2003).

We must emphasize that no strong seismic evidence was found in all the seismic experiments performed in North-Iberia up to date for the presence of a slab of oceanic crust sinking into the mantle towards the south. Even models considering “oceanic subduction” like the one by Álvarez-Marrón et al. (1998) represent in fact an “oceanic underthrusting” beneath the margin, a geometry imposed by the shallow position and gently dipping of the Moho observed in the wide-angle data. Only Ayarza et al. (2004) interpreted two diverging subcrustal reflectors found in the marine ESCIN-3.2 and ESCIN-3.3 seismic reflection profiles (west of the area covered by the MARCONI profiles; see location in Figure 1) as reflections produced at the top of a southward-subducting slab. However, these authors had to assume a subducting slab with a high curvature, that seems difficult to justify from a geodynamic point of view, in order to match the arrivals of these divergent reflections in a 3D ray-tracing modeling. Also, the presence of other deep reflectors with different inclinations (e.g. in the eastern part of the ESCIN-3.3 profile) would require a complex folded and/or broken geometry for the subducted slab (Álvarez-Marrón et al., 1996).

More recently, Roca et al. (2011) have assumed that the layer of 7.2-7.3 km/s found at the base of the crust in the western part of the MARCONI survey area corresponds to

serpentinized upper mantle in the footwall of the extensional detachment that led to the exhumation of the upper mantle. According to these authors, the subsequent compression along North-Iberia produced not only the subduction to the north of the Iberian lower-middle crust clearly observed inland, but also the contractional reactivation of the extensional detachment, leading to a southward-directed subduction of the serpentinized upper mantle approximately beneath the northern front of the Le Danois bank. This interpretation is hardly compatible with the results presented here and with previous results for the ESCIN-4 profile (Pulgar et al., 1996; Gallart et al., 1997; Fernández-Viejo et al., 1998) because the level of 7.2-7.3 km/s is continuous in this area, showing a very gentle slope all the way to the coastline and beyond. An additional difficulty for this interpretation is to explain the nature of the interface at the base of this level and on top of the one with velocities as low as 7.8-7.9 km/s (or even 7.5-7.7 km/s in the wedge located on top of the Iberian crustal root), where sharp Moho-like reflections are observed.

6.4. General interpretation: distinctive rifted margin domains

The Bay of Biscay has been used recently as a natural laboratory to develop and apply an approach to characterize and identify distinctive rifted margin domains, both offshore and in land outcrops (Tugend et al., 2014, 2015). In this section we discuss the association of zones A, B and C defined in the previous sections with the proximal, necking, hyperthinned, exhumed mantle and oceanic domains proposed by Tugend et al. (2014, 2015). However, the fact that the original Mesozoic domains were modified to different degrees by the Cenozoic contractional deformation makes this association relatively complex.

Zone A comprises areas with Moho depths around ~30 km and areas with significant crustal thinning, with Moho depths ranging from ~30 to ~20 km. North and West of the Landes High, crustal thicknesses less than 20 km are related to the hyperthinned domain. According to the definition by Tugend et al. (2014, 2015) the boundary between the necking and the hyperthinned domains would be placed at the point where the whole crust is fully coupled and brittle, allowing faults to penetrate into the mantle. Along MARCONI-1, this point was placed at the distal part of the slope in the Mesozoic margin but, subsequent contractional deformation piled up the whole hyperthinned domain into the accretionary wedge, as also pointed out by Tugend et al., (2014). South of the accretionary wedge, the necking domain is characterized by a progressive thickening, with the Moho being located around 30 km depth close to the coastline. Proximal domains are characterized by weak to no

838 rift-related lithosphere and crustal thinning, and can hold graben and half graben basins with
839 low stretching factors (Tugend et al., 2014, 2015). These features are observed in a ~50-60
840 km-wide strip following the coastline, where the Variscan crust was less affected by the later
841 tectonic events. However, this region is more properly associated with the necking domain as
842 before the Cenozoic contractional deformation its thickness was less than ~30 km (Pedreira et
843 al., 2015). The original proximal domain corresponded to the Mesozoic continental platform,
844 which extended along and to the south of the present-day central Cantabrian Mountains. The
845 eastern part of the Cantabrian Mountains, on the other hand, were formed by the inversion of
846 the Basque-Cantabrian Basin, which was another hyperextended rift arm with its own
847 necking, hyperthinned and exhumed mantle domains (Tugend et al., 2014; DeFelipe et al.,
848 2017). Zone C, therefore, comprises the whole range of Mesozoic rift domains, later inverted
849 to build up the Cantabrian Mountains.

850
851 From the edge of the accretionary prism to the north, Zone B can be associated to the
852 exhumed mantle domain, although we must note that to the south, the high velocity basal
853 layer of this domain is underthrust beneath the hyperthinned and necking domains. As clear
854 reflectors are identified on top and bottom of the high-velocity lower crustal layer and the
855 seismic velocities do not increase significantly with depth, the high velocities in the lower
856 crust can hardly be associated to mantle material with a decreasing degree of serpentinization
857 with depth. On the contrary, those high velocities can be related to intrusions of mafic rocks
858 in a partially exhumed and serpentinized mantle. In the original definition of “exhumed
859 mantle domain” by Tugend et al. (2014, 2015), the top of the basement is considered to be
860 composed of mantle rocks, although local remnants of continental crust may be preserved as
861 extensional allochthons on top of it. In the area covered by the MARCONI profiles, we
862 interpret that serpentinized mantle do not form the top of the basement, but constitutes a well
863 defined layer at the base of the crust, covered by a very thin layer with typical upper crustal
864 velocities. We think that, despite this difference, the same terminology of “exhumed mantle
865 domain” can be used for this area of the Bay of Biscay, but considering that mantle
866 exhumation was only partial. Total mantle exhumation is expected to occur to the west, from
867 ~6°W to 8°W, where M0-M3 anomalies were interpreted to be created by serpentinized
868 exhumed mantle (Sibuet et al., 2007). Finally, the oceanic domain, marked by the clear
869 presence of A33o and A34 anomalies, is located further west (westward of 8°W), outside of
870 the area investigated here (Sibuet et al. 2004).

7. Conclusions

The results derived from the wide angle modeling of the most representative profiles acquired during the MARCONI project show the high structural complexity of the Bay of Biscay and the northern sector of the Iberian Peninsula. This complexity results from the extensional processes occurred during the Mesozoic, producing the opening of the Bay of Biscay, and the Tertiary Alpine compressional phase that produced the partial closure of the bay, an intense deformation of the North-Iberian margin and the building of the Pyrenean-Cantabrian mountain belt.

Models derived from the wide-angle phases recorded at the N-S profiles prove that the complex deep structure involving crustal imbrication clearly imaged beneath the Pyrenees, extends continuously to the west along the Basque-Cantabrian basin and the Cantabrian Mountains. The models for the southern sector of the MARCONI N-S profiles allow to continuously constrain the indentation of the Bay of Biscay and Iberian crusts, resulting in the subduction to the north of the Iberian middle and lower crusts.

Offshore, the N-S and E-W profiles show an important crustal thinning to the North and to the West. This diminution of the crustal thickness is particularly important in the north-westernmost sector of the study region, where the crust is 10-15 km thick and shows high velocities in the lower crust preceded by anomalously low velocities in the upper layers. The velocity depth distributions in this area, corresponding to the distal part of the margin and the abyssal plain, do not show the typical characteristics of either continental or oceanic crust. The decrease in crustal thickness is controlled by the loss of a well-defined middle crust, disrupting the continental structure observed inland. The lower crust shows high velocities (7.2-7.3 km/s) and moderate thinning in comparison with the upper layers. However, multichannel seismic profiles show numerous normal faults and half-graben structures, typical of continental extensional processes, and clear magnetic anomalies associated to oceanic seafloor spreading are not observed within the area. The velocity structure also differs from the one usually observed in other magma-poor rifted margins, such as the northern segment of the West Iberia margin, in which high velocity zones with strong velocity gradients are explained by progressive mantle serpentinization. Although the resolution of the Marconi seismic experiment is not enough to reach strong conclusions on this particular topic, we hypothesize that mafic igneous intrusions resulting from decompression melting in the mantle could have been added to the base of the crust and top of serpentinized mantle,

explaining the layer with rather constant thickness, seismic velocities of 7.2-7.3 km/s and PmP reflections at its base. It would correspond to an “exhumed mantle domain” (Tugend et al., 2014) in which exhumation was not complete, since remnants of a highly stretched upper continental crust are interpreted to overlay the serpentinized mantle.

The crustal structure depicted from the velocity-depths models obtained in the easternmost sector of the study region (the marine area bordered by the Capbreton, Cap Ferret and Santander canyons) shows the typical pattern of continental crust. In this area the crustal thinning is not as marked as in the western sector but an important reduction of the crustal thickness to the north is observed, always conserving the continental crust properties. The margin Moho is located around 30 km depth to the south of the Capbreton canyon (proximal domain) and thins to ~20 km across the necking domain up to the northern part of the Landes High and the Parentis Basin. This is consistent with previous results from the ECORS-Bay of Biscay profile, which imaged an important crustal thinning when crossing the Parentis basin, interpreted as an hyperthinned domain (Tugend et al., 2014). To the west of this sector, the Moho is rather flat at depths close to 20 km, but rises again from the middle point of MARCONI-4 profile towards the west, connecting with the exhumed mantle domain of the NW sector of the study region.

Acknowledgements

This work was carried out with the support of the MARCONI (REN2001-1734) project from Spanish MCYT. M.R. benefited from a PhD from the Spanish MCYT. This work was supported also by the Consolider-Ingenio 2010 Programme, under project CDS2006-0041 “Topo-Iberia”, TopoMed CGL2008-03474-E/BTE and Spanish Ministry of Economy and Competitiveness Project MISTERIOS (CGL2013-48601-C2-2-R). We thank the Institut de Physique du Globe de Paris for providing the grid of magnetic anomalies in the Bay of Biscay. We gratefully acknowledge Martin Schimmel for providing his code of the frequency-dependent lateral phase coherence filter and his support in the improvement of the final record-sections.

References:

- Aller, J. and Zeyen, H.J. (1996). A 2.5D interpretation of the Basque country magnetic anomaly (northern Spain): geodynamical implications. *Geol. Rundsch.*, 85, 303-309.
- Alonso, J.L., Pulgar, J.A., García-Ramos, J.C. and Barba, P. (1996). Tertiary basins and Alpine tectonics in the Cantabrian mountains (NW Spain). A: *Tertiary basins of Spain: The Stratigraphic Record of Crustal Kinematics*, edited by Friend P.F. and Dabrio, C.J., pp. 214-227, Cambridge University Press, Cambridge.
- Álvarez-Marrón, J., Pérez-Estaún, A., Dañobeitia, J.J., Pulgar, J.A., Martínez Catalán, J.R., Marcos, A., Bastida, F., Ayarza-Arribas, P., Aller, J., Gallart, J., Gonzalez-Lodeiro, F., Banda, E., Comas, M.C. and Córdoba, D. (1996). Seismic structure of the northern continental margin of Spain from ESCIN deep seismic profiles. *Tectonophysics*, 264, 153-174.
- Álvarez-Marrón, J., Rubio, E. and Torné, M. (1997). Subduction-related structures in the North Iberian Margin. *J. Geophys. Res.* V. 102, NO. B10, pp. 22,497-22,511.
- Ardizzone, J., Mezcua, J. and Socías, I. (1989). Mapa aeromagnético de España Peninsular, Instituto Geográfico Nacional, Madrid.
- Ayarza, P., Martínez-Catalán, J.R., Gallart, J., Pulgar, J.A and Dañobeitia, J.J. (1998). Estudio Sísmico de la Corteza Ibérica Norte 3.3: A seismic image of the Variscan crust in the hinterland of the NW Iberian Massif. *Tectonics*, v. 17, No. 2, 171-186.
- Ayarza, P., Martínez-Catalán, J.R., Álvarez-Marrón, J., Zeyen, H. and Juhlin, C. (2004). Geophysical constraints on the deep structure of a limited ocean-continent subduction zone at the North Iberian Margin. *Tectonics*, V. 23, pp. 1-21.
- Beaumont, C., Muñoz, J.A., Hamilton, J. and Fullsack, P. (2000). Factors controlling the Alpine evolution of the central Pyrenees inferred from a comparison of observations and geodynamical models. *J. Geophys. Res* V. 105, N. B4, pp. 8121-8145.
- Barnett Moore, Nicholas, Dietmar R Müller, Simon Williams, Jakob Skogseid, and Maria Seton. "A Reconstruction of the North Atlantic Since the Earliest Jurassic." *Basin Research*, September 1, 2016. doi:10.1111/bre.12214.
- Boillot, G., and R. Capdevila, The Pyrenees: Subduction and collision?, *Earth Planet. Sci. Lett.*, 121(5), 151–160, 1977.
- Boillot, G. and J. Malod (1988). The north and northwest Spanish continental margin: a review. *Rev. Soc. Geol. España*, 1, 295-316.

- 972 Boillot, G., Féraud, G., Recq, M., and Girardeau, J. (1989). "Undercrusting" by serpentinite
973 beneath rifted margins: the example of the west Galicia margin (Spain). *Nature*, 341:523-
974 525.
- 975 Bois, C., Pinet, B. and Gariel, O. (1997). The sedimentary cover along the ECORS Bay of
976 Biscay deep seismic reflection profile. A comparison between the Parentis basin and other
977 European rifts and basins. *Mém. Soc. Géol. France*, n. 171, 143-165.
- 978 Bronner, A., Sauter, D., Manatschal, G., Péron-Pinvidic, G., Munschy, M. (2011). Magmatic
979 breakup as an explanation for magnetic anomalies at magma-poor rifted margins *Nature*
980 *Geoscience* 4 (8), 549-553
- 981 Brun, J. P., and Beslier, M. O. (1996). Mantle exhumation at passive margins. *Earth Planet.*
982 *Sci. Lett.*, 142(1), 161-173.
- 983 Capdevila, R., G. Boillot, C. Lepvrier, J. A. Malod, and G. Mascle (1980), Les formations
984 cristallines du Banc Le Danois (marge nord-iberique), *C. R. Acad. Sci.*, Ser. D, 291, 317–
985 320.
- 986 Casas, A., Kearey, P., Rivero, L. and Adam, C.R. (1997). Gravity anomaly map of the
987 Pyrenean region and a comparison of the deep geological structure of the western and
988 eastern Pyrenees. *Earth and Planet. Sci. Lett.*, 150, 65-78.
- 989 Chevrot, S., Sylvander, M., Diaz, J., Ruiz, M. Paul, A. and the PYROPE Working Group
990 (2015). The Pyrenean architecture as revealed by teleseismic P-to-S converted waves
991 recorded along two dense transects. *Geophys. J. Int.*, 200, 1096-1107. doi:
992 10.1093/gji/ggu400
- 993 Chian, D., Loudon, K.E., Minshull, T.A. and Whitmarsh, R.B. (1999), Deep structure of the
994 ocean-continent transition in the southern Iberia Abyssal Plain from seismic refraction
995 profiles: The Ocean Drilling Program (Legs 149 and 173) transect, *J. Geophys. Res.*, 104:
996 7443-7462.
- 997 Cho, H.M., Kim, H.J., Jou, H.T., Hong, J.K. and Baag, C.E., (2004). Transition from rifted
998 continental to oceanic crust at the south-eastern Korean margin in the East Sea (Japan Sea).
999 *Geophys. Res. Lett.* V. 31, L07606, doi:10.1029/2003GL019107.
- 1000 Choukroune, P. (1992). Tectonic Evolution of the Pyrenees. *Annu. Rev. Earth Planet. Sci.* 20,
1001 143-158.
- 1002 Choukroune, P. and Etude Continentale et Océanique par Reflexion et Refracción Sísmique
1003 (ECORS) Team, (1989). The ECORS Pyrenean deep seismic profile reflection data and the
1004 overall structure of an orogenic belt. *Tectonics*, 8, 23-39.
- 1005 Christensen, N.I. and Mooney, W.D. (1995). Seismic velocity structure and composition of
1006 the continental crust: A global view. *J. Geophys. Res.* V. 100, No. B7, pp. 9761-9788.

1007 Daignières, M., Gallart, J. and Banda, E. (1981). Lateral variation of the crust in the North
1008 Pyrenean Zone. *Ann. Geophys.* 37,3, 435-456.

1009 Daignières, M., Gallart, J., Banda, E. and Hirn, A. (1982). Implications of the seismic
1010 structure for the orogenic evolution of the Pyrenean range. *Earth and Planet. Sci. Lett.*, 57,
1011 88-100.

1012 Daignières, M., de Cabissole, B., Gallart, J., Hirn, A., Suriñach, E. and Torné, M.. (1989).
1013 Geophysical constraints on the deep structure along the ECORS Pyrenees Line. *Tectonics*,
1014 V. 8, N. 5, 1051-1058.

1015 Daignières, M., Séguet, M., Specht, M. and ECORS team. (1994). The Arzacq-Western
1016 Pyrenees ECORS deep seismic profile. *Publ. Eur. Assoc. Pet. Geol.* 4, 199-208.

1017 Dean, S. M., Minshall, T. A., Whitmarsh, R. B., & Loudon, K. E. (2000). Deep structure of
1018 the ocean-continent transition in the southern Iberia Abyssal Plain from seismic refraction
1019 profiles: The IAM-9 transect at 40° 20' N. *J. Geophys. Res.: Solid Earth* (1978–2012),
1020 105(B3), 5859-5885. doi: 10.1029/1999JB900301

1021 DeFelipe, I., Pedreira, D., Pulgar, J. A., Iriarte, E. and Mendiá, M. (2017). Mantle exhumation
1022 and metamorphism in the Basque-Cantabrian Basin (N Spain). Stable and clumped isotopic
1023 analysis in carbonates and comparison with ophicalcites in the North-Pyrenean Zone
1024 (Urdach and Lherz). *Geochem. Geophys. Geosyst.*, doi 10.1002/2016GC006690.

1025 Díaz, J., Gallart, J., Pedreira, D., Pulgar, J.A., Ruiz, M., López, C. and González-Cortina, J.M.
1026 (2003). Teleseismic imaging of alpine crustal underthrusting beneath N Iberia. *Geophys.*
1027 *Res. Lett.*, 30, 11, 1554, doi:10.1029/2003GL017073.

1028 Diaz, J., Gallart, J., Pulgar, J.A., Ruiz, M., Pedreira, D., 2009. Crustal structure beneath
1029 North-West Iberia imaged using receiver functions. *Tectonophysics* 478, 175–183.
1030 doi:10.1016/j.tecto.2009.08.003

1031 Díaz, J., Pedreira, D., Ruiz, M., Pulgar, J.A., and Gallart, J. (2012). Mapping the indentation
1032 between the Iberian and Eurasian plates beneath the Western Pyrenees/Eastern Cantabrian
1033 Mountains from receiver function analysis. *Tectonophysics*, V. 570–571, pp, 114–122, doi:
1034 10.1016/j.tecto.2012.07.005.

1035 Díaz, J., Gallart, J. and Carbonell R. (2016). Moho topography beneath the Iberian-Western
1036 Mediterranean region mapped from controlled-source and natural seismicity surveys.
1037 *Tectonophysics*, doi: 10.1016/j.tecto.2016.08.02.

1038 Fernández-Viejo, G., Gallart, J., Pulgar, J.A., Gallastegui, J., Dañobeitia, J.J. and Córdoba, D.
1039 (1998) Crustal transition between continental and oceanic domains along the North Iberian
1040 margin from wide angle seismic and gravity data. *Geophys. Res. Lett.* v. 25. No. 23, pp.
1041 4249-4252.

1042 Fernández-Viejo, G., Gallart, J., Pulgar, J.A., Córdoba, D. and Dañobeitia, J.J. (2000).
 1043 Seismic signature of Variscan and Alpine tectonics in NW Ibèria: Crustal structure of the
 1044 Cantàbrian Mountains and Duero basin. *J. Geophys. Res.* V. 105, NO. B2, 3001-3018.
 1045 Fernández-Viejo, G., Gallastegui, J., Pulgar, J.A. and Gallart, J. (2011). The MARCONI
 1046 reflection seismic data: A view into the eastern part of the Bay of Biscay. *Tectonophysics*,
 1047 508, 34-41, doi:10.1016/j.tecto.2010.06.020.
 1048 Fernández-Viejo, G., Pulgar, J.A., Gallastegui, J., Quintana, L., (2012). The Fossil
 1049 Accretionary Wedge of the Bay of Biscay: Critical Wedge Analysis on Depth-Migrated
 1050 Seismic Sections and Geodynamical Implications. *The Journal of Geology*, 120, 315–331.
 1051 Ferrer, O., Roca, E., Benjumea, B., Muñoz, J.A.; Ellouz, N. and the MARCONI Team. (2008).
 1052 The deep seismic reflection MARCONI-3 profile: Role of extensional Mesozoic structure
 1053 during the Pyrenean contractional deformation at the eastern part of the Bay of Biscay.
 1054 *Mar. Petr. Geol.* V. 25, pp 714-730.
 1055 Fillon, C., D. Pedreira, P. A. van der Beek, R. S. Huisman, L. Barbero, and J. A. Pulgar
 1056 (2016), Alpine exhumation of the central Cantabrian Mountains, Northwest Spain,
 1057 *Tectonics*, 35, doi:10.1002/2015TC004050.
 1058 Gallart, J. Daignières, M., Banda, E., Suriñach, E. and Hirn, A. (1980). The eastern Pyrenean
 1059 domain: lateral variations at crust-mantle level. *Ann. Géophys.*, 36 (2), 141-158.
 1060 Gallart, J., Banda, E. and Daignières, M., (1981). Crustal structure of the Paleozoic Axial
 1061 Zone of the Pyrenees and transition to the North Pyrenean Zone. *Ann. Géophys*, 37, 3, 457-
 1062 480.
 1063 Gallart, J., Fernández-Viejo, G., Díaz, J., Vidal, N. and Pulgar, J.A. (1997). Deep structure of
 1064 the transition between the Cantabrian mountains and the North Iberian Margin from wide-
 1065 angle ESCI-N data. *Rev. Soc. Geol. España*, 8 (4), 1995, 365-382.
 1066 Gallastegui, J. (2000), Estructura cortical de la cordillera y margen continental cantabricos:
 1067 Perfiles ESCI-N, *Trab. Geol.*, 22, 234.
 1068 Gallastegui, J., Pulgar, J.A. and Álvarez-Marrón, J. (1997). 2-D seismic modelling of the
 1069 Variscan foreland thrust and fold belt crust in NW Spain from ESCIN-1 deep seismic
 1070 reflection data. *Tectonophysics*, 269, 21-32.
 1071 Gallastegui, J. Pulgar, J. A. and Gallart, J. (2002). Initiation of an active margin at North
 1072 Iberian continent-ocean transition. *Tectonics*, 21, No.4, doi:10.1029/2001TC901046.
 1073 Gallastegui, J., Pulgar, J. A., and Gallart, J. (2016) Alpine tectonic wedging and crustal
 1074 delamination in the Cantabrian Mountains (NW Spain), *Solid Earth*, 7, 1043-1057,
 1075 doi:10.5194/se-7-1043-2016.
 1076 García-Mondéjar, J., Agirrezala, L.M., Aranburu, A., Fernández-Mendiola, P.A., Gómez-

1077 Pérez. I., López-Horgue, M. and Rosales, I. (1996), Aptian-Albian tectonic pattern of the
 1078 Basque-Cantabrian Basin (Northern Spain). *Geol. Jour.* V. 31., 13-45.

1079 Gómez, M., Vergés, J. and Riaza, C. (2002). Inversion tectonics of the northern margin of the
 1080 Basque Cantabrian Basin. *Bull. Soc. Géol. France.* t. 173, n. 5, pp. 449-459.

1081 Jabaloy, A. Galindo-Zaldívar, J. González-Lodeiro, F. (2002). Paleostress evolution of the
 1082 Iberian Península (Late Carboniferous to present-day). *Tectonophysics*, 357. 159-186.

1083 Jammes, S., Manatschal, G., Lavier, L., Masini, E., (2009). Tectono-sedimentary evolution
 1084 related to extreme crustal thinning ahead of a propagating ocean: the example of the
 1085 western Pyrenees. *Tectonics* 28, TC4012, <http://dx.doi.org/10.1029/2008TC002406>

1086 Jammes, S., R. S. Huismans, and J. A. Muñoz (2014), Lateral variation in structural style of
 1087 mountain building: Controls of rheological and rift inheritance, *Terra Nova*, 26, 201–207,
 1088 doi:10.1111/ter.12087.

1089 Jones E.W. and Ewing, J.I. (1969). Age of the Bay of Biscay; evidence from seismic profiles
 1090 and bottom samples. *Science*, 166, 102-105.

1091 Korenaga, J., Holbrook, W.S., Kent, G.M., Kelemen, P.B., Detrick, R.S. Larsen, H.C.,
 1092 Hopper, J.R. and Dahl-Jensen, T. (2000). Crustal structure of the southeast Greenland
 1093 margin from joint refraction and reflection seismic tomography. *J. Geophys. Res.*, 105,
 1094 21,591-21,614.

1095 Lagabrielle, Y., Bodinier, J.-L., 2008. Submarine reworking of exhumed subcontinental
 1096 mantle rocks: Field evidence from the Lherz peridotites, French Pyrenees. *Terra Nova* 20,
 1097 11–21.

1098 Lagabrielle, Y., Labaume, P., de Saint Blanquat, M., 2010. Mantle exhumation, crustal
 1099 denudation, and gravity tectonics during Cretaceous rifting in the Pyrenean realm (SW
 1100 Europe): Insights from the geological setting of the lherzolite bodies. *Tectonics*, 29,
 1101 TC4012, [http:// dx.doi.org/10.1029/2009TC002588](http://dx.doi.org/10.1029/2009TC002588).

1102 Le Borgne, E., Le Mouél, J-L. and Le Pichon, X. (1971): Aeromagnetic survey of South-
 1103 western Europe, *EPSL*, 12: 287-299.

1104 Loudeiro, A., Afilhado, A., Matias, L., Moulin, M. and Aslanian, D., 2016. Monte Carlo
 1105 approach to assess the uncertainty of wide-angle layered models: Application to the Santos
 1106 Basin, Brazil. *Tectonophysics*, 683, 286-307.

1107 Marillier, F., Tomassino, A., Priat, Ph and Pinet, B. (1988). Deep structure of the Aquitaine
 1108 Shelf: constraints from expanding spread profiles on the ECORS Bay of Biscay transect.
 1109 *Mar. Pet. Geol.* V. 5, 65-74.

- 1110 Martín-González, F., Heredia, N., 2011. Complex tectonic and tectonostratigraphic evolution
1111 of an Alpine foreland basin: The western Duero Basin and the related Tertiary
1112 depressions of the NW Iberian Peninsula. *Tectonophysics* 502, 75–89.
- 1113 Martínez-Catalan, J.R, Ayarza-Arribas, P., Pulgar, J.A., Pérez-Estaún., A., Gallart, J.,
1114 Marcos., A., Bastida., F., Álvarez-Marrón, J., González-Lodeiro, F., Aller, J., Dañobeitia,
1115 J.J., Banda, E., Córdoba., D. and Comas, M.C. (1997). Results from the ESCI-N3.3 marine
1116 deep seismic profile along the Cantabrian continental margin. *Rev., Soc. Geol. España*, 8
1117 (4), 1995, 341-354.
- 1118 Mattauer, M. (1990). Une autre interprétation du profil ECORS Pyrénées. *Bull. Soc. Géol.*
1119 *France*, Serie 8, 6 (2), 307-311.
- 1120 Minshull, T.A. (2002). Seismic structure of the oceanic crust and passive continental margins.
1121 Invited contribution to "*The IASPEI International handbook of earthquake and*
1122 *engineering seismology*", Vol. 81A. Edited by Lee, W.H.K., Kanamori, H., Jennings, P.C.
1123 and Kisslinger, C. Academic Press, London. Pp. 911-924.
- 1124 Mihoubi, A., Schnürle, P., Benaissa, Z., Badsì, M., Bracene, R., Djelit, H., Geli, L., Sage, F.,
1125 Agoudjil, A. and Klingelhoefer, F., 2014. Seismic imaging of the eastern Algerian margin
1126 off Jijel: integrating wide-angle seismic modelling and multichannel seismic pre-stack
1127 depth migration. *Geophys. J. Int.*, 198, 1486-1503.
- 1128 Montigny, R., Azambre, B., Rossy, M., Thuizat, R (1986). K-Ar study of Cretaceous
1129 magmatism and metamorphism in the Pyrenees: age and length of rotation of the Iberian
1130 Peninsula. *Tectonophysics*, 129, 257-273.
- 1131 Mooney, W.D., Prodehl, C. and Pavlenkova, N.I. (2002). Seismic velocity structure of the
1132 continental lithosphere from controlled source data. Invited contribution to "*The IASPEI*
1133 *International handbook of earthquake and engineering seismology*", Vol. 81A. Edited by
1134 Lee, W.H.K., Kanamori, H., Jennings, P.C. and Kisslinger, C. Academic Press, London.
1135 Pp. 887-910.
- 1136 Moulin, M., Klingelhoefer, F., Afilhado, A., Allanian, D., Schnurle, Ph., Nouze, H.,
1137 Rabineau, M., Beslier, M.-O. and Feld, A. 2015. Deep crustal structure across a young
1138 passive margin from wide-angle and reflection seismic data (The SARDINIA Experiment)
1139 – I. Gulf of Lion's margin. *Bull. Soc. Geol. France*, 186, 4-5, 309-330.
- 1140 Mouthereau, F., Filleaudeau, P.Y., Vacherat, A., Pik, R., Lacombe, O., Fellin, M.G.,
1141 Castelltort, S., Christophoul, F., Masini, E., 2014. Placing limits to shortening evolution in
1142 the Pyrenees: Role of margin architecture and implications for the Iberia/Europe
1143 convergence. *Tectonics*. doi:10.1002/2014TC003663
- 1144 Muñoz, J.A. (1992). Evolution of a continental collision belt: ECORS- Pyrenees crustal

1145 balanced cross-section. McClay, K.R. (Editor) *Thrust Tectonics*. Chapman and Hall.
1146 London, 235-246.

1147 Pedreira, D., Pulgar, J.A., Gallart, J. and Díaz, J. (2003). Seismic evidence of Alpine crustal
1148 thickening and wedging from the Western Pyrenees to the Cantabrian Mountains (North
1149 Iberia). *J. Geophys. Res.* Vol. 108, N. B4, 2204, doi 10.1029/2001JB001667.

1150 Pedreira, D., Pulgar, J. A., Gallart, J., and Torné, M. (2007). Three-dimensional gravity and
1151 magnetic modeling of crustal indentation and wedging in the western Pyrenees-Cantabrian
1152 Mountains. *J. Geophys. Res.* Vol. 112. B12405, doi:10.1029/2007JB005021.

1153 Pedreira, D., Afonso, J.C., Pulgar, J.A., Gallastegui, J., Carballo, A., Fernández, M., García-
1154 Castellanos, D., Jiménez-Munt, I., Semprich, J., (2015). Geophysical petrological
1155 modeling of the lithosphere beneath the Cantabrian Mountains and North-Iberian margin:
1156 geodynamic implications. *Lithos* 230, 46–68. doi.org/10.1016/j.lithos.2015.04.018.

1157 Pérez-Estaún, A., Bastida, F., Alonso, J. L., Marquínez, J., Aller, J., Álvarez-Marrón, J.,
1158 Marcos, A. and Pulgar, J.A., (1988). A thin-skinned tectonics model for an arcuate fold
1159 and thrust belt: the Cantabrian Zone (Variscan Ibero-Armorican Arc). *Tectonics*, 7: 517-
1160 537.

1161 Pérez-Estaún, A., Pulgar, J.A., Banda, E., Álvarez-Marrón, J. and ESCI-N Research Group.
1162 (1994). Crustal structure of the external variscides in northwest Spain from deep seismic
1163 reflection profiling. *Tectonophysics*, 232, 91-118.

1164 Pérez-Gussinyé, M., J.P. Morgan, T.J Reston & C.R. Ranero (2006), From rifting to
1165 spreading at non-volcanic margins: insights from numerical modeling. *Earth Planet. Sci.*
1166 *Lett.*, 244, 458-473, doi:10.1016/j.epsl.2006.01.059.

1167 Péron-Pinvidic, G., and G. Manatschal (2009). The final rifting evolution at deep
1168 magma-poor passive margins from Iberia-Newfoundland: A new point of view. *Int. J.*
1169 *Earth Sci.*, 98(7), 1581-1597. doi:10.1007/s00531-008-0337-9.

1170 Pickup, S.L.B., Whitmarsh, R.B., Fowler, C.M.R. and Reston, T.J. (1996). Insight into the
1171 nature of the ocean-continent transition off West Iberia from deep multichannel seismic
1172 reflection profile. *Geology*, v. 24, n. 12, 1079-1082.

1173 Pous, J., Queralt, P. and Marcuello, A. (2001). Magnetotelluric signature of the western
1174 Cantabrian Mountains. *Geophys. Res. Lett.* V. 28, No. 9, 1795-1798.

1175 Pulgar, J.A., Gallart, J., Fernández-Viejo, G., Pérez-Estaún, A., Álvarez-Marrón, J. and
1176 ESCIN Group. (1996). Seismic image of the Cantabrian Mountains in the western
1177 extension of the Pyrenees from integrated ESCIN reflection and refraction data.
1178 *Tectonophysics*, 264, 1-19.

1179 Pulgar, J.A., Pérez-Estaún, A., Gallart, J., Álvarez-Marrón, J., Gallastegui, J., Alonso, J.L.
 1180 and ESCIN Group (1997). The ESCI-N2 deep seismic reflection profile: a traverse across
 1181 the Cantabrian Mountains and adjacent Duero basin. *Rev. Soc. Geol. España*, 8 (4), 1995,
 1182 383-394.

1183 Rat, P. (1988). The Basque-Cantabrian basin between the Iberian and European plates; some
 1184 facts but still many problems. *Rev. Soc. Geol. Esp.* 1 (3-4): 327-348.

1185 Reston, T.J. (2009), The structure, evolution and symmetry of the magma-poor rifted margins
 1186 of the North and Central Atlantic: A synthesis, *Tectonophysics*, 468: 6–27,
 1187 doi:10.1016/j.tecto.2008.09.002.

1188 Roca, E., Muñoz, J.A., Ferrer, O. and Ellouz, N. (2011). The Role of the Bay of Biscay
 1189 Mesozoic extensional structure in the configuration of the Pyrenean orogeny: Constraints
 1190 from the MARCONI deep seismic reflection survey. *Tectonics*. V. 30, TC2001, doi:
 1191 10.1029/2010TC002735.

1192 Roure, F., Choukroune, P., Berastegui, X., Muñoz, J.A., Villien, A., Matheron, P., Bareyt, M.,
 1193 Seguret, M., Camara, P. and Deramond, J. (1989). ECORS deep seismic data and balanced
 1194 cross sections: geometric constraints on the evolution of the Pyrenees. *Tectonics*, V. 8, No.
 1195 1, pp. 41-50.

1196 Rudnick, R.L. and Fountain, D.M. (1995). Nature and composition of the continental crust: A
 1197 lower crustal perspective. *Reviews of Geophysics*, 33, 3. 267-309.

1198 Ruppel, C. (1995). Extensional processes in continental lithosphere. *J. Geophys. Res.* V. 100,
 1199 No. B12, 24,187-24,215

1200 Sawyer, D.S., Coffin, M.F., Reston, T.J., Stock, J.M., Hopper, J.R. (2007), COBBOOM: The
 1201 Continental Breakup and Birth of Oceans Mission. *Scientific Drilling*, No. 5, September
 1202 2007.

1203 Schimmel, M. and Gallart, J. (2007). Frequency-dependent phase coherence for noise
 1204 suppression in seismic array data. *J. Geophys. Res.* Vol. 112, B04303, doi:
 1205 10.1029/2006JB004680.

1206 Séguret M. and Daignières, M. (1986). Crustal scale balanced cross-sections of the Pyrenees;
 1207 discussion, *Tectonophysics*, 129, 303-318.

1208 Sibuet, J.C., Srivastava, S.P. and Spakman, W. (2004). Pyrenean orogeny and plate
 1209 kinematics. *J. Geophys. Res.*, 109, B08104, doi:10.1029/2003JB002514.

1210 Sibuet, J. C., S. Srivastava, and G. Manatschal (2007), Exhumed mantle-forming transitional
 1211 crust in the Newfoundland-Iberia rift and associated magnetic anomalies, *J. Geophys. Res.*,
 1212 112, B06105, doi:10.1029/2005JB003856.

1213 Srivastava, S.P., Schouten, H., Roest, W.R., Klitgord, K.D., Kovacs, L.C., Verhoef, J. and
1214 Macnab, R. (1990). Iberian plate kinematics: A jumping boundary between Eurasia and
1215 Africa, *Nature*, 344, 756-759.

1216 Srivastava, S. P. and Roest, W. R. (1999). Extent of oceanic crust in the Labrador Sea. *Mar.*
1217 *Pet. Geol.*, 16 (1), 65-84.

1218 Suriñach, E. Marthelot, J.M., Gallart, J., Daignières, M. and Hirn, A. (1993). Seismic images
1219 and evolution of the Iberian Crust in the Pyrenees. *Tectonophysics*, 221, 67-80.

1220 Teixell A. (1998). Crustal structure and orogenic material budget in the west central Pyrenees.
1221 *Tectonics*, 17(3), pp. 395-406. *Comptes Rendus Geosciences*, 348, 257-267, doi:
1222 10.1016/j.crte.2015.10.010

1223 Teixell A., Labaume, P and Lagabriele, Y. (2016). The crustal evolution of the west-central
1224 Pyrenees revisited: Inferences from a new kinematic scenario.

1225 Thinon, I., Matias, L., Réhault, J.P., Hirn, A., Fidalgo-González, L. and Avedik, F. (2003).
1226 Deep structure of the Armorican Basin (Bay of Biscay): a review of Norgasis seismic
1227 reflection and refraction data. *J. Geol. Soc. Lond.*, V. 160, pp. 99-116.

1228 Tucholke, B.E., Austin Jr, J.A. & Uchupi, E., 1989. Crustal structure and rift-drift evolution
1229 of the Newfoundland Basin, in *Extensional tectonics and stratigraphy of the North Atlantic*
1230 *Margins*, pp. 247–263, eds Tankard, A.J. & Balkwill, H.R., American Association of
1231 Petrology and Geology , Tulsa.

1232 Tugend, J., G. Manatschal, N. J. Kusznir, E. Masini, G. Mohn, and I. Thinon (2014),
1233 Formation and deformation of hyperextended rift systems: Insights from rift domain
1234 mapping in the Bay of Biscay- Pyrenees, *Tectonics*, 33, 1239–1276,
1235 doi:10.1002/2014TC003529.

1236 Tugend, J., G. Manatschal, N. J. Kusznir and E. Masini (2015), Characterizing and identifying
1237 structural domains at rifted continental margins: application to the Bay of Biscay margins
1238 and its Western Pyrenean fossil remnants. *Geol. Soc. London, Special Publ.* 413: 171-203.
1239 doi:10.1144/SP413.3

1240 Turner, J.P. (1996). Switches in subduction direction and the lateral termination of mountain
1241 belts: Pyrenees-Cantabrian transition, Spain. *Jour. Geol. Soc.* Vol. 153. 563-571.

1242 Van der Voo, R. (1990), Phanerozoic paleomagnetic poles from Europe and North America
1243 and comparison with continental reconstructions, *Rev. Geophys.*, 18, 167–206.

1244 Vergés, J., Millán, H., Roca, E., Muñoz, J.A., Marzo, M., Cirés, J., Den Bezemer, T.,
1245 Zoetemeijer, R. and Cloetingh, S. (1995). Eastern Pyrenees and related foreland basins:
1246 Pre-, syn- and post-collisional crustal-scale cross-sections. *Mar. Pet. Geol.*, 12, pp. 893-
1247 915.

1248 Wang, Y., Chevrot, S., Monteiller, V., Komatitsch, D., Mouthereau, F., Manatschal, G.,
1249 Sylvander, M., Diaz, J., Ruiz, M., Grimaud, F., Benahmed, S., Pauchet and Martin, R.
1250 (2016). The deep roots of the western Pyrenees revealed by full waveform inversion of
1251 teleseismic P waves. *Geology*, doi:10.1130/G37812.1

1252 White, S.R., McKenzie, D. and O’Nions, K.R., (1992). Oceanic crustal thickness from
1253 seismic measurements and rare element inversions. *J. Geophys. Res.* V. 97. No B13,
1254 19.683-19.715.

1255 Whitmarsh, R. B., and Sawyer, D. S. (1996). The ocean/continent transition beneath the Iberia
1256 Abyssal Plain and continental-rifting to seafloor-spreading processes. In *Proceedings of*
1257 *the Ocean Drilling Program, Scientific Results*, Eds. Whitmarsh, R.B., Sawyer, D.S.,
1258 Klaus, A., and Masson, D.G. Vol. 149. pp. 713-736.

1259 Zelt, C.A. (1999). Modelling strategies and model assessment for wide-angle seismic
1260 traveltimes data. *Geophys. J. Int.*, 139, 183-204.

1261 Zelt, C.A. and Smith, R.B. (1992). Seismic traveltimes inversion for 2-D crustal velocity
1262 structure, *Geophys. J. Int.*, 108, 16-34.

1263

1264

1265

Figure captions:

Figure 1. a) Tectonic map of Northern Iberia and the Bay of Biscay showing the location of MARCONI profiles and the previous seismic profiles acquired in the area. Triangles represent land seismic stations, circles OBS and OBH instruments and blue lines the shooting profiles, with the wider lines identifying the profiles discussed in detail. A, B and C, designate the three crustal domains differentiated in section 6 of this work. Offshore magnetic map from Le Borgne et al. (1971); trace of magnetic anomalies A34, M0 and M3 from Sibuet et al. (2004). b) Bouguer anomaly map of the same area (data from Bureau Gravimétrique International). Bathymetric contours each 250 m. TC: Torrelavega canyon. SC: Santander canyon. CFC: Cap Ferret canyon. CBC: Capbreton canyon. LC: Lastres canyon. LLC: Llanes canyon

Figure 2.- Results for the N-S MARCONI-1 profile, OBS/OBH stations. a) OBH20 record section acquired at the hydrophone channel and ray tracing over the final velocity depth model. Only the marine sector of the model is shown. Theoretical travel times and rays from waves propagated across the sediments and the upper crust are shown in red. Travel times and rays from waves propagated across the deeper regions of the Bay of Biscay crust are shown in green. b) Same panels for OBS08.

Figure 3.- Results for the N-S MARCONI-1 profile, land stations. a) Record section for the vertical channel of station B3. The ray tracing along the final velocity model and theoretical travel times are shown using the same red and green code as in Figure 2. Travel times and rays of waves propagated across the Iberian middle and lower crust are shown in blue. Data from station B3 allow to constrain the velocity of the upper mantle beneath the Bay of Biscay. b) Same panels for the B6 land station. The PcP_I and PmP_I seismic phases, related to reflections at the top and bottom of the Iberian lower crust, are clearly imaged.

Figure 4.- N-S MARCONI-3 Profile. Modeling results for OBS16 (a) and D2 land station (b), both constraining the crustal structure beneath the Bay of Biscay. c) Results for the D7 land station, where phases related to the deep structure of the Iberian crust are detected (PcP_I and PmP_I phases depicted in blue).

Figure 5.- E-W Profile MARCONI-4. a) Modeling results obtained in the eastern sector (OBS18), sampling a thinned continental crust. b) Results for OBS19, located at the abyssal plain and constraining the transitional crust in the western sector on the profile. c) Results for OBS04, sampling the thinned structure of the western edge of the investigated area. Pn phases detected at offsets of 90-130 km reveal a low-velocity upper mantle.

Figure 6.- Velocity-depth model for the profiles discussed in the text. Bold lines show the interface segments constrained by the data. The recording sites are displayed in white triangles and the vertical discontinuous black lines show the crossing points between profiles. a) N-S MARCONI-1. In this case, the Bouguer anomaly observations (dashed line) and the model of Pedreira et al. 2015 (red line) are included for reference. b) N-S MARCONI-3. c) E-W MARCONI-4

Figure 7- Three-dimensional view of the crustal models in the Bay of Biscay. In the eastern sector, a crustal thinning to the north and to the west is revealed, but the continental character of the crust is preserved. In the western sector, the Moho is located above 20 km and the lower crust and upper mantle show, respectively, high and low velocities. This is interpreted as corresponding to a transitional stage between continental and oceanic crustal structures.

Figure 8.- 1D P-wave velocity-depth profiles obtained in the eastern (green) and western (red) sectors of the Bay of Biscay. Black line shows the reference average crustal model of Christensen and Mooney (1995) and blue line shows the 1D velocity-depth model at the inland zone of the Marconi01 profile (km 30 in Figure 6). Light blue area shows the velocity-depth distributions range of Atlantic oceanic crust for ages between 59-127 Ma (White et al., 1992). Light purple area marks the range of velocities found in the ocean-continental transition of the West Iberia Margin, where exhumed and serpentinized mantle has been drilled (Chian et al., 1999; Dean et al., 2000).

Supplementary Material

Supplementary Figure S1: Examples of pre-processing of the OBS/H and land stations data. A) Record section of the OBS16 (profile 3 N-S) after a time and offset-dependent frequency filtering and a Wiener deconvolution. Ormsby band-pass filter in the ranges 3-5-12-17 Hz and 3-5-8-12 Hz has been applied for offsets smaller and greater than 105 km, respectively. B) The same OBS seismic section after adding an F-K filtering and a frequency-dependent lateral phase coherence filter (Schimmel and Gallart, 2007). C) Record section of the D1 land station (profile 3 N-S) after applying a 3-15 Hz Butterworth band-pass filter. D) Same section after applying a frequency-dependent lateral phase coherence filter.

Supplementary Figure S2: Results for MARCONI profiles 5 (a) and 8 (b). Upper panels show the final velocity-depth models. Middle and bottom panels show the record section and the modeled ray tracing, with theoretical travel times and rays from waves propagated across the sediments and the upper crust in red and those from waves propagated across the deeper regions in green.

Supplementary Figure S3: Velocity-depth models for the main profiles discussed in the text. Dark shadings show ray paths from the modeling and hence the area which can be considered as constrained by data. The velocity-depth grids have been clipped to the well-constrained area. a) NS MARCONI-1, b) N-S MARCONI-3, c) E-W MARCONI-4

Figure 1 (with caption below and on the same page)

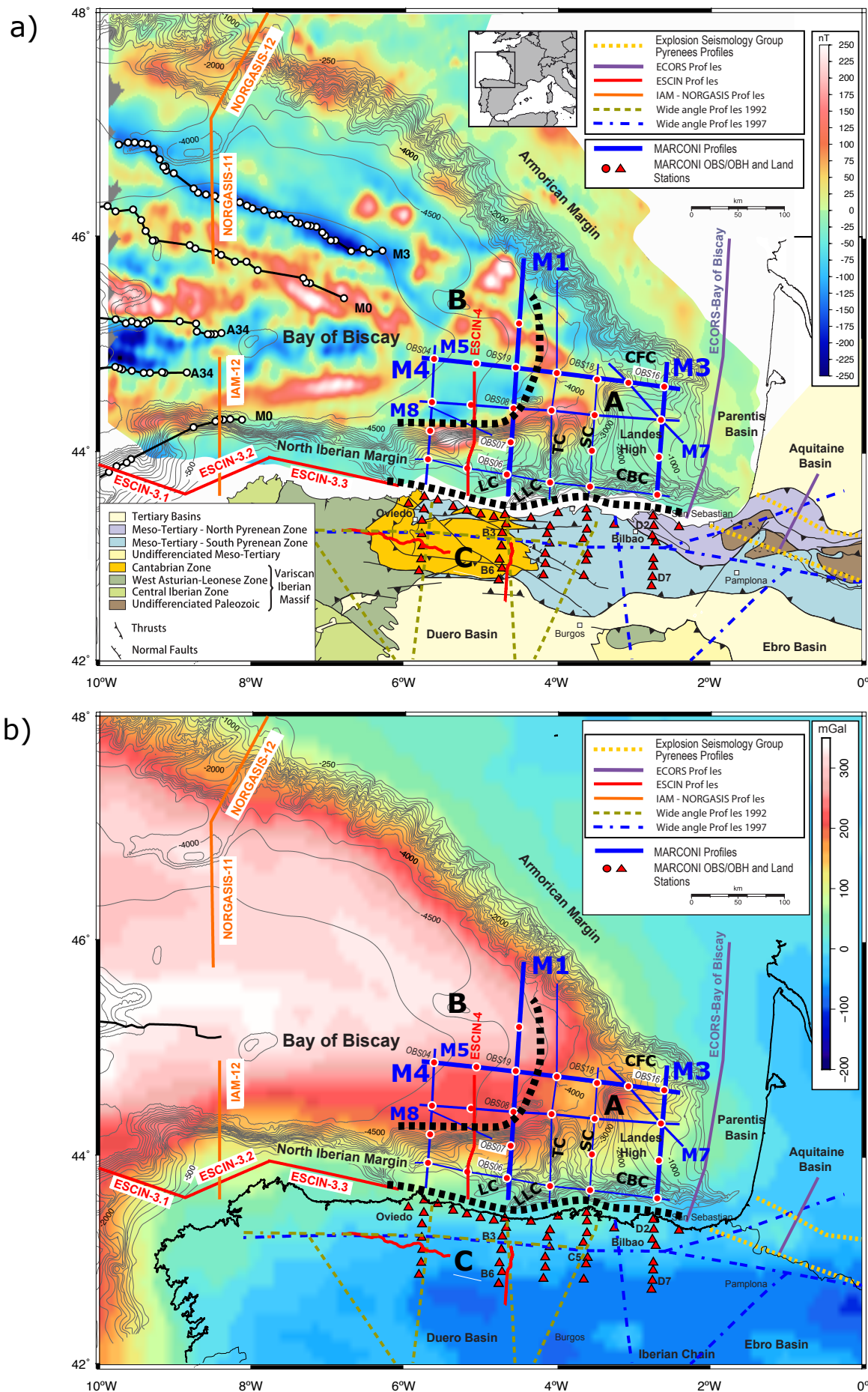


Figure 1: a) Tectonic map of Northern Iberia and the Bay of Biscay showing the location of MARCONI profiles and the previous seismic profiles acquired in the area. Triangles represent land seismic stations, circles OBS and OBH instruments and blue lines the shooting profiles, with the wider lines identifying the profiles discussed in detail. A, B and C, designate the three cortical domains differentiated in section 6 of this work. Offshore magnetic map from Le Borgne et al. (1971); trace of magnetic anomalies A34, M0 and M3 from Sibuet et al., (2004). b) Bouguer anomaly map of the same area (data from Bureau Gravimétrique International). Bathymetric contours each 250 m. TC: Torrelavega canyon. SC: Santander canyon. CFC: Cap Ferret canyon. CBC: Capbreton canyon. LC: Lastres canyon. LLC: Llanes canyon.

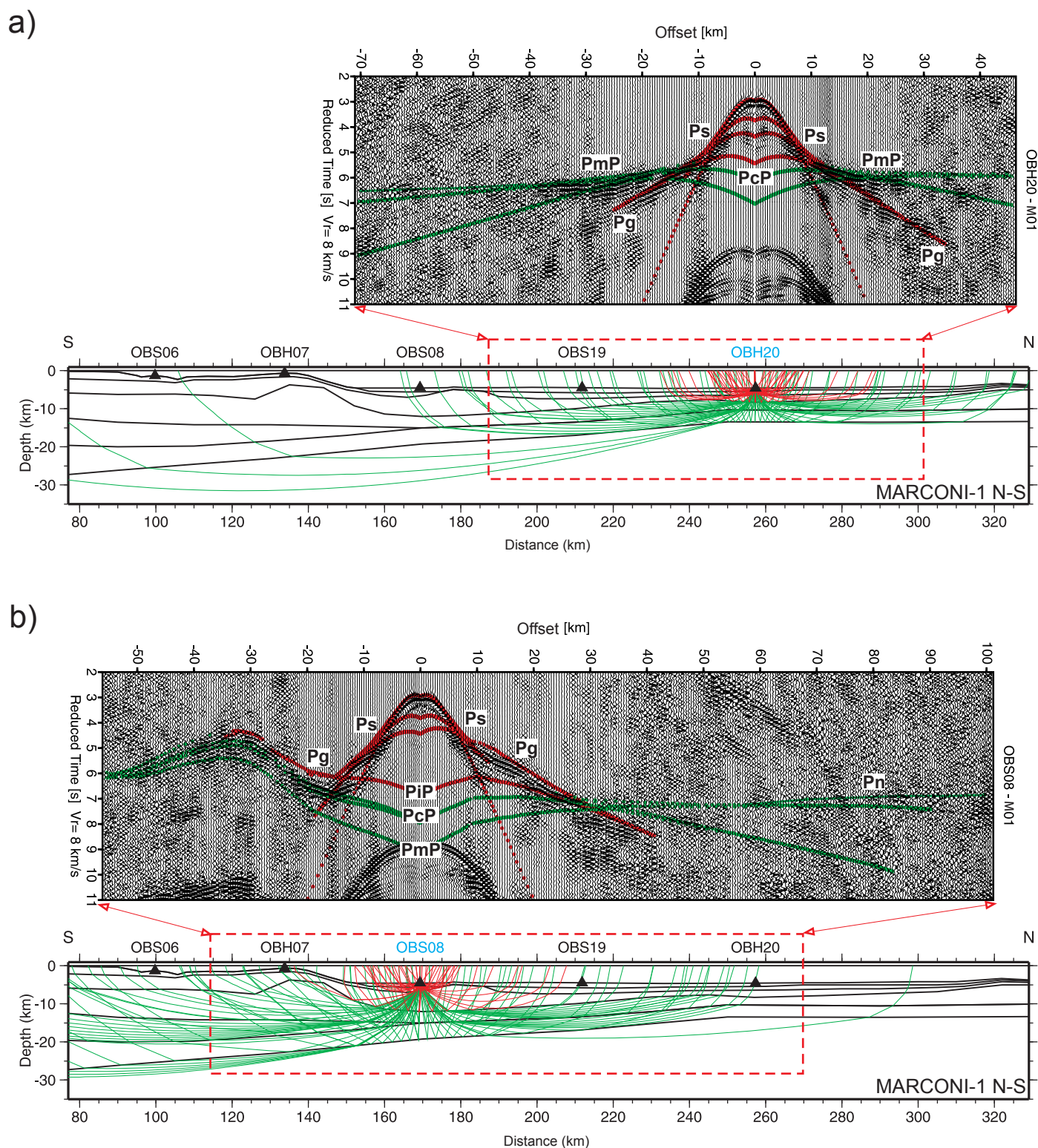


Figure 2: Results for the N-S MARCONI-1 profile, OBS/OBH stations. a) OBH20 record section acquired at the hydrophone channel and ray tracing over the final velocity depth model. Only the marine sector of the model is shown. Theoretical travel times and rays from waves propagated across the sediments and the upper crust are shown in red. Travel times and rays from waves propagated across the deeper regions of Bay of Biscay are shown in green. b) Same panels for OBS08.

Figure 3 (with caption below and on the same page)

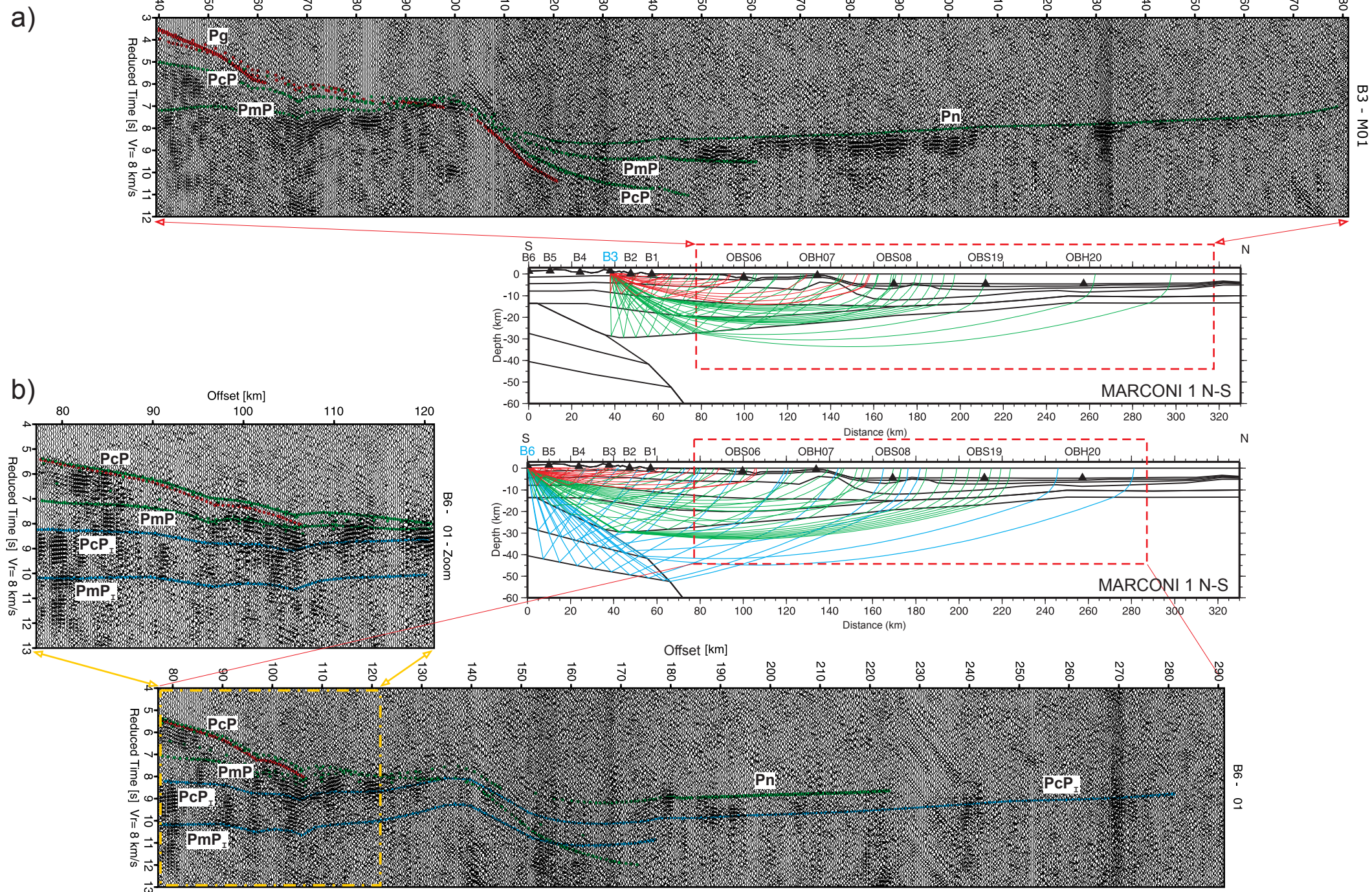


Figure 3: Results for the N-S MARCONI-1 profile, land stations. a) Record section for the vertical channel of station B3. The ray tracing along the final velocity model and the theoretical travel times are shown using the same red and green code as in Figure 2. Travel times and rays of waves propagated across the Iberian middle and lower crust are shown in blue. Data from station B3 allow to constrain the upper mantle velocity beneath the Bay of Biscay. b) Same panels for station B6. The PcP1 and PmP1 phases, related to reflections at the top and base of the Iberian lower crust are clearly imaged.

Figure 4 (with caption below and on the same page)

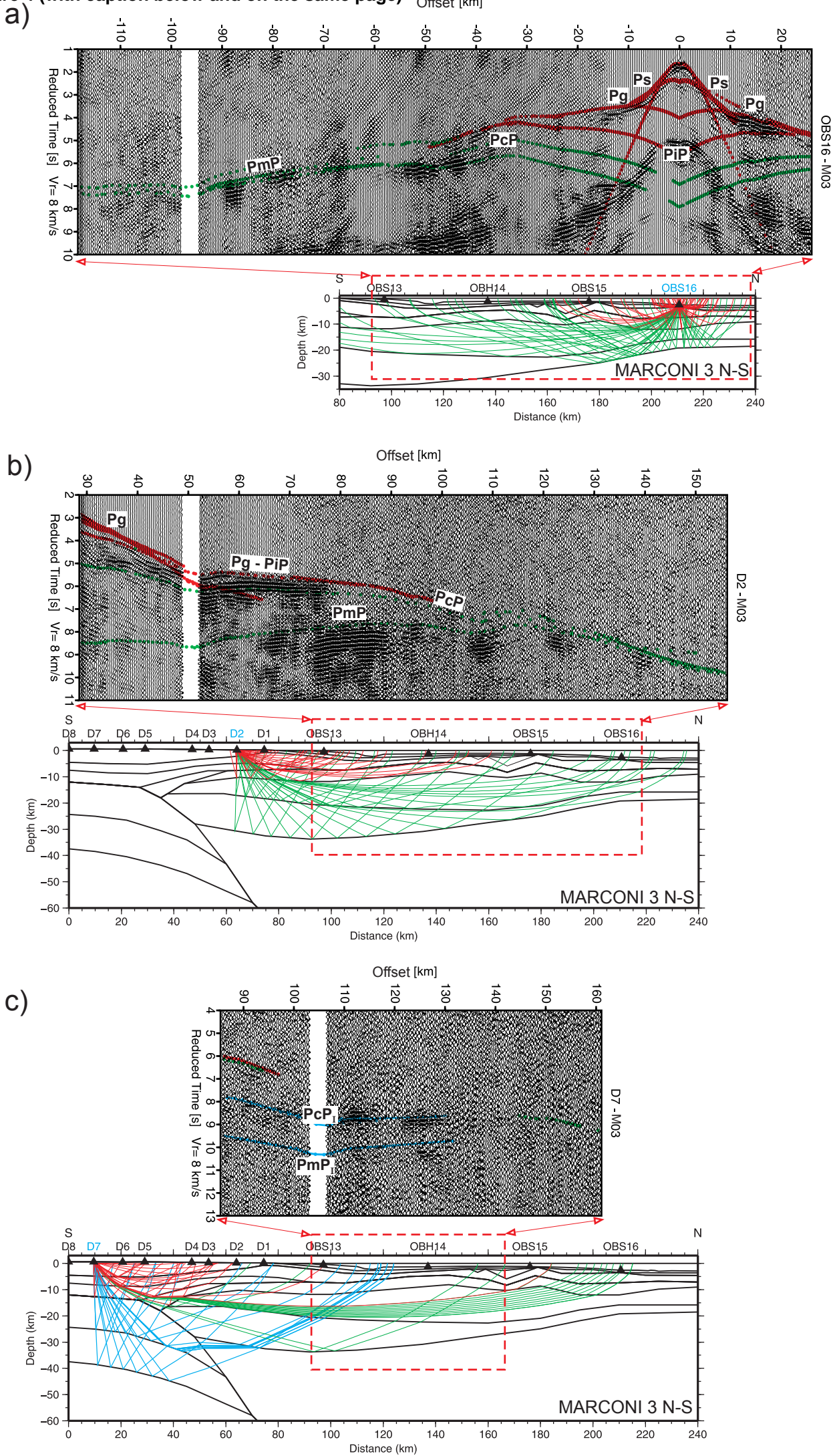


Figure 4: N-S MARCONI-3 profile. Modelling results for OBS16 (a) and land station D2 (b), both constraining the crustal structure beneath the Bay of Biscay. c) Results for the D7 land station, where phases related to the deep structure of the Iberian crust are detected.

Figure 5 (with caption below and on the same page)

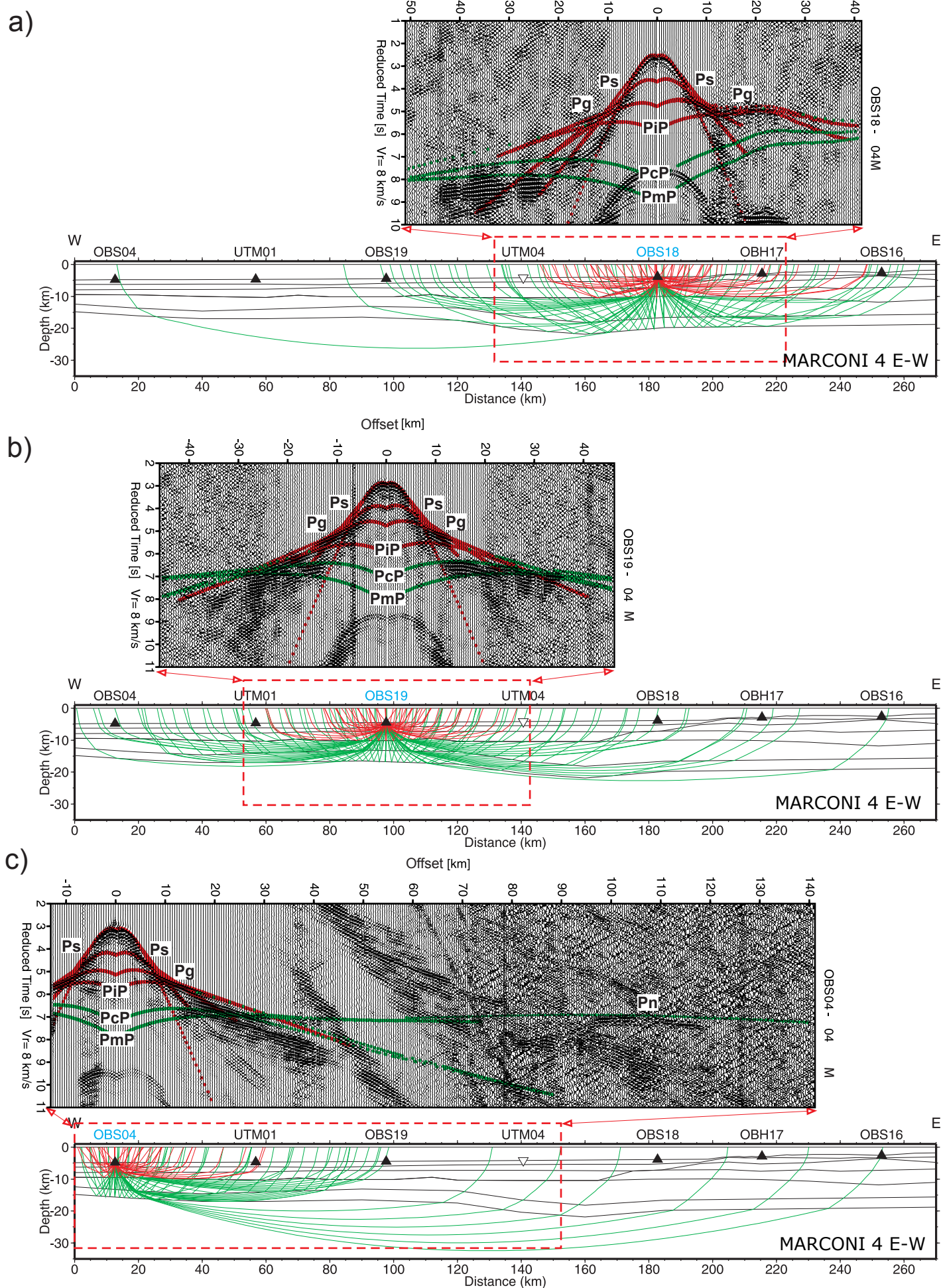


Figure 5: E-W profile MARCONI-4. a) Modeling results obtained in the eastern sector (OBS18) sampling a thinned continental crust. b) Results for OBS19, located at the abyssal plain and constraining the transitional crust in the western sector of the profile. c) Results for OBS04, sampling the thinned crust of the western edge of the investigated area. Pn phases detected at offsets of 90-130 km reveal a low velocity in the upper mantle.

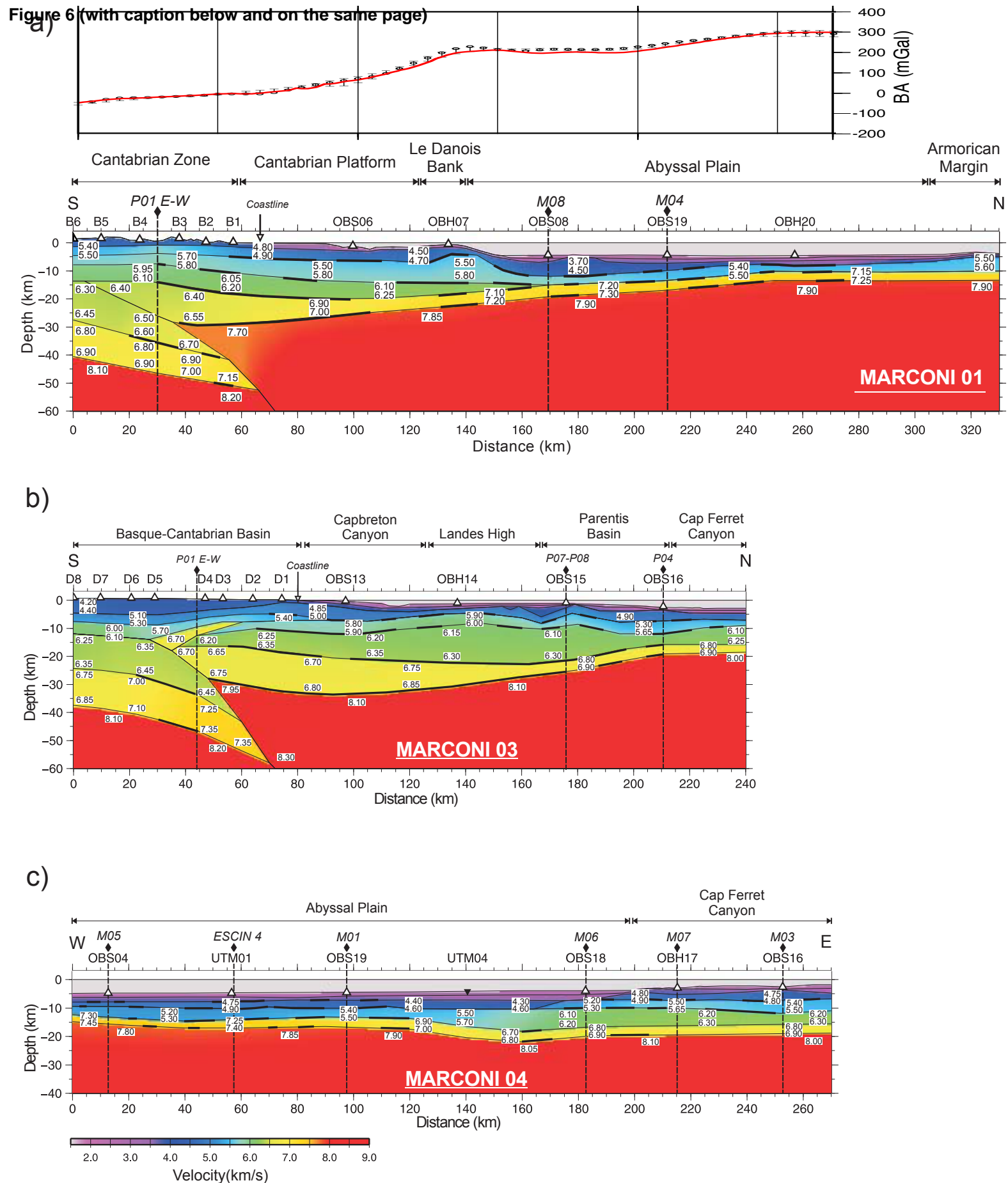


Figure 6: Velocity-depth models for the profiles discussed in the text. Bold lines show the interface segments constrained by data. The recording sites are displayed in white triangles and the vertical dashed black lines show the crossing points between profiles. a) NS MARCONI-1. In this case, the Bouguer anomaly observations (dashed line) and model of Pedreira et al. 2015 (red line) are included for reference, b) N-S MARCONI-3 and c) E-W MARCONI-4.

Figure 7 (with caption below and on the same page)

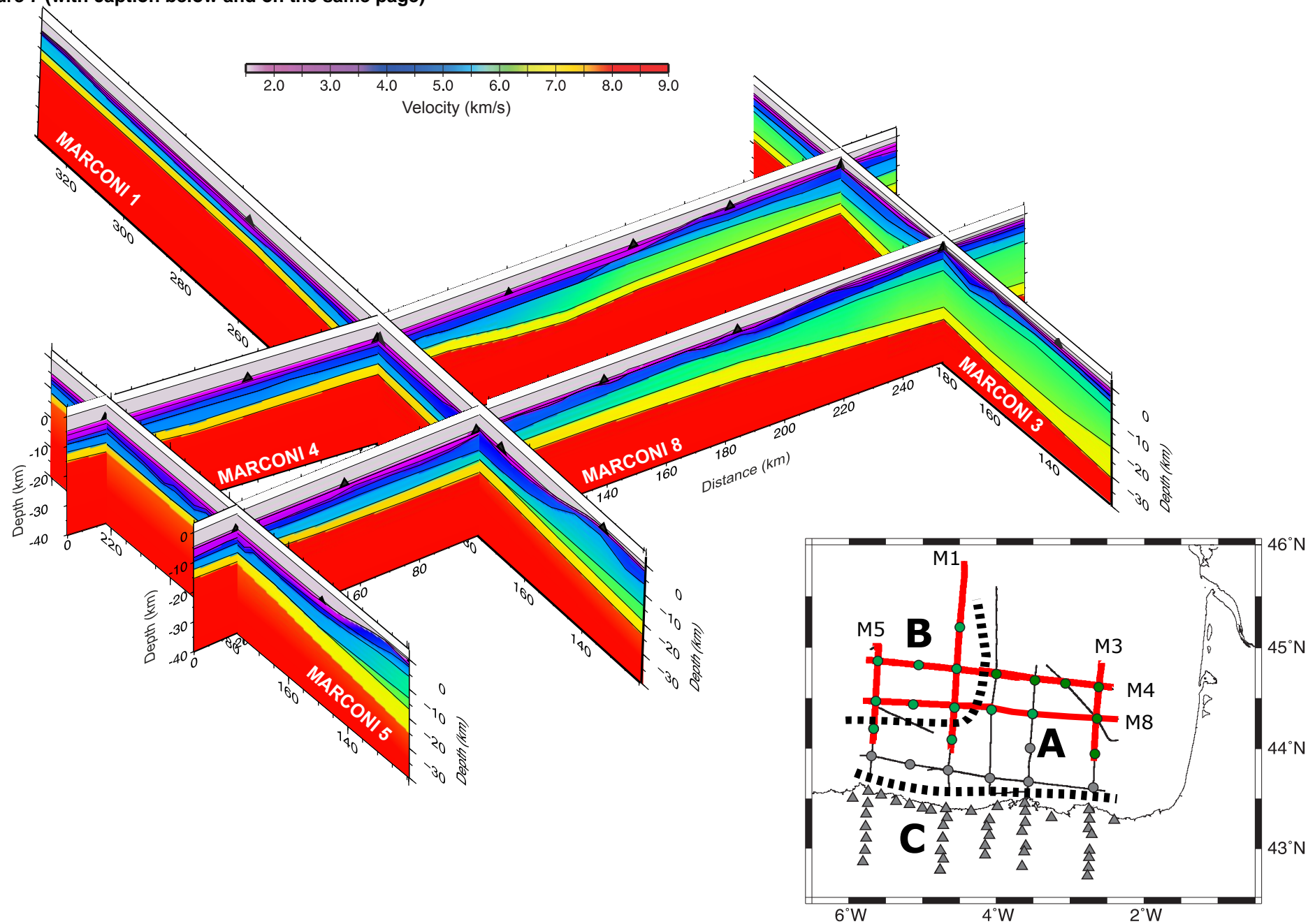


Figure 7: Three dimensional view of the crustal models in the Bay of Biscay. In the eastern sector a crustal thinning to the North and to the West is revealed, but the continental character of the crust is preserved. In the western sector the Moho is located above 20 km and the lower crust and the uppermost mantle show, respectively, high and low velocities. This is interpreted as corresponding to a transitional stage between continental and oceanic crustal structures.

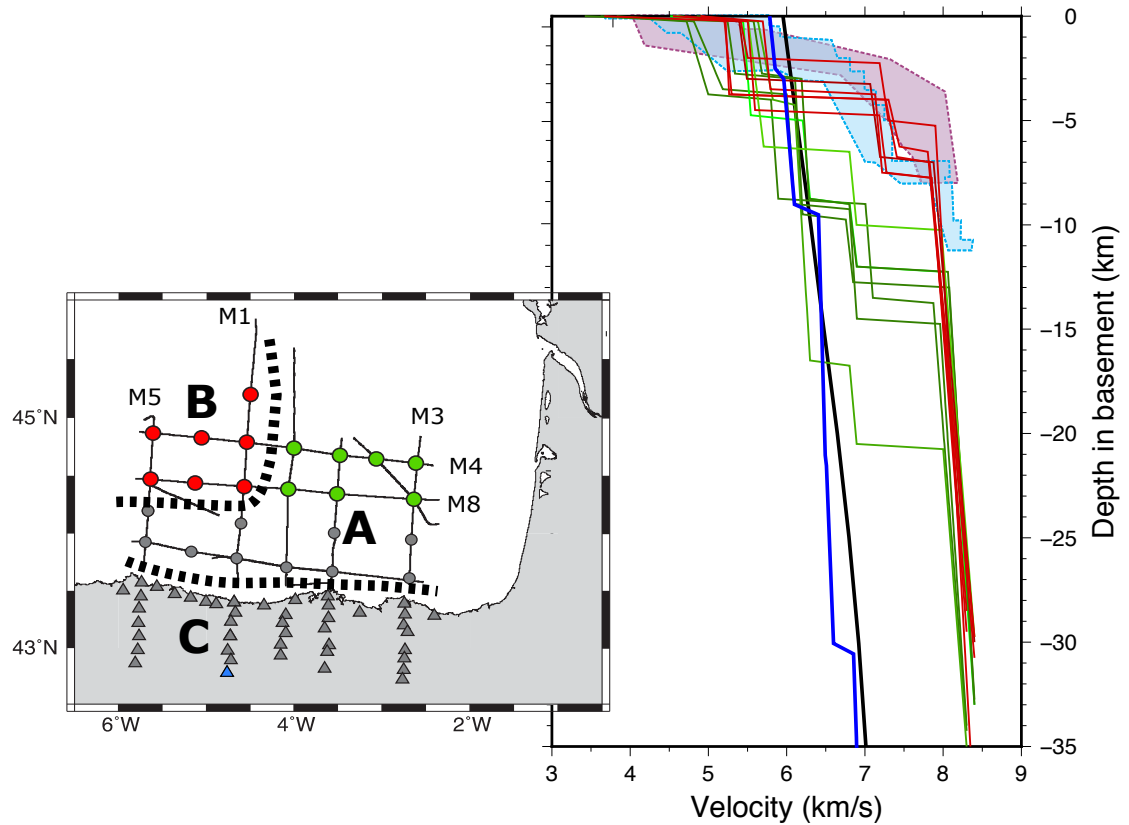


Figure 8: 1D P-wave velocity-depth profiles obtained in the eastern (green) and western (red) sectors of the Bay of Biscay. Black line shows the reference average crustal model of Christensen and Mooney (1995) and blue line shows the 1D velocity-depth profile at the inland zone of the Marconi01 profile (km 30 in Figure 6). Light blue area shows the velocity-depth distributions range of Atlantic oceanic crust for ages between 59-127 Ma (White et al., 1992). Light purple area marks the range of velocities found in the ocean-continental transition of the West Iberia Margin, where exhumed and serpentinized mantle has been drilled (Chian et al., 1999; Dean et al., 2000).